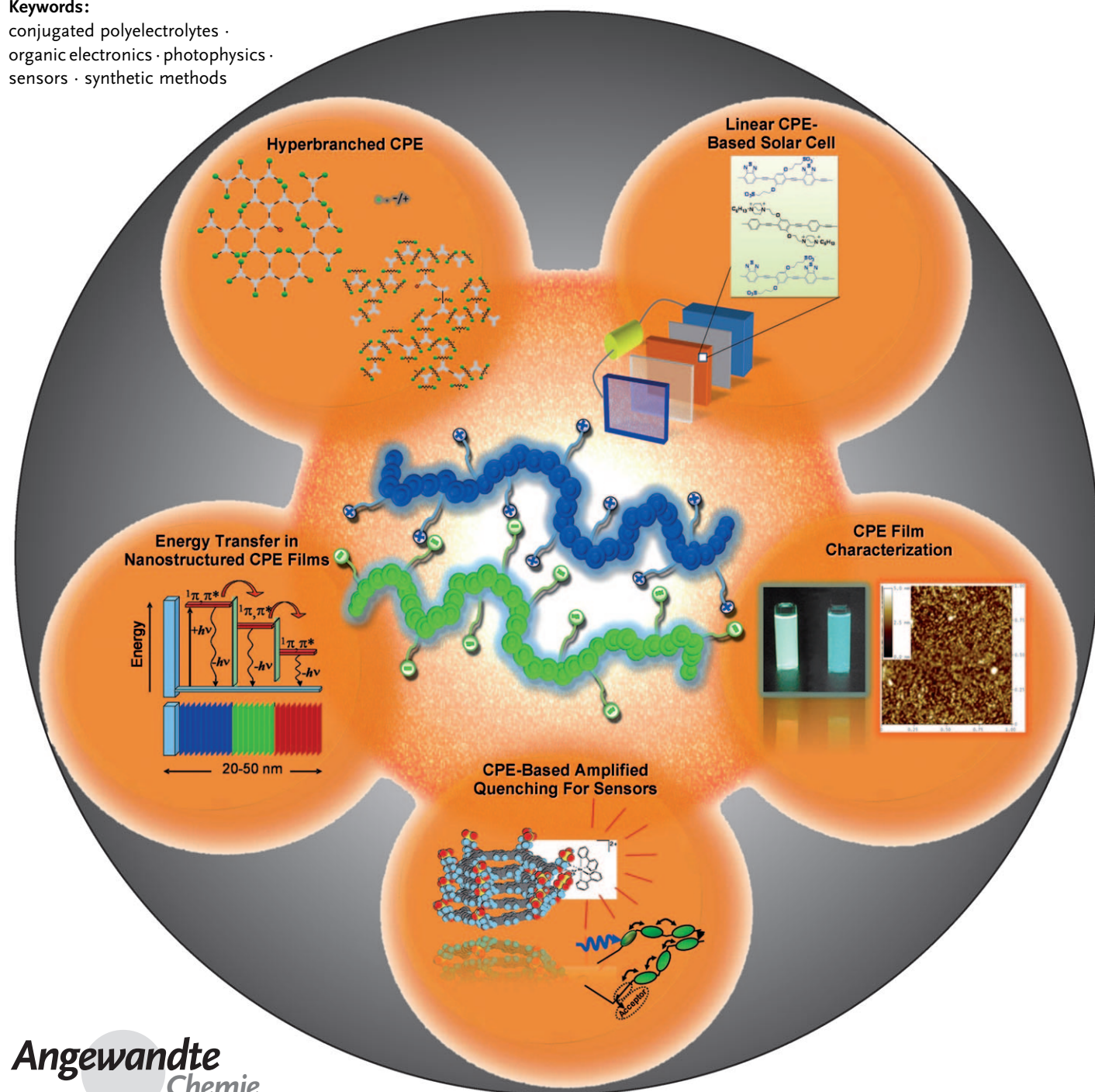


# Conjugated Polyelectrolytes: Synthesis, Photophysics, and Applications

Hui Jiang, Prasad Taranekar, John R. Reynolds,\* and Kirk S. Schanze\*

## Keywords:

conjugated polyelectrolytes · organic electronics · photophysics · sensors · synthetic methods



**O**rganic optoelectronic polymers have evolved to the point where fine structural control of the conjugated main chain, coupled with solubilizing and property-modifying pendant substituents, provides an entirely new class of materials. Conjugated polyelectrolytes (CPEs) provide a unique set of properties, including water solubility and processability, main-chain-controlled exciton and charge transport, variable band gap light absorption and fluorescence, ionic interactions, and aggregation phenomena. These characteristics allow these materials to be considered for use in applications ranging from light-emitting diodes and electrochromic color-changing displays, to photovoltaic devices and photodetectors, along with chemical and biological sensors. This Review describes the evolution of CPE structures from simple polymers to complex materials, describes numerous photophysical aspects, including amplified quenching in macromolecules and aggregates, and illustrates how the physical and electronic properties lead to useful applications in devices.

## 1. Introduction

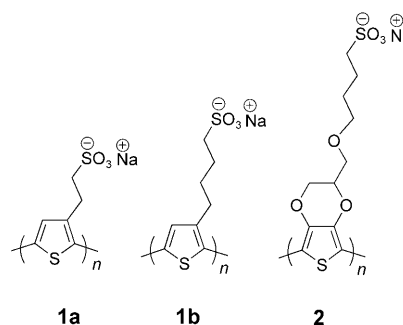
Conjugated polymers have been developed into a class of materials that provide structurally controllable properties ranging from high conductivity in redox-doped states to light emission for light-emitting diodes, light absorption for solar cells and electrochromic devices, charge transport for organic electronics,  $\pi$ -electron polarization for nonlinear optics, and chemical sensitivity for use in chemo- and bio-sensors.<sup>[1,2]</sup> Although early compositions of conjugated polymers tended to be poorly soluble and infusible, making processing to useful structures difficult or impossible, polymer chemists have conquered these limitations by various approaches such that many useful materials are now available for both research and commercial applications. For example, poly(3,4-ethylenedioxythiophene)/poly(styrenesulfonate) (PEDOT/PSS), poly(3-alkyl thiophene)s, and polyanilines are now prepared on a commercial scale. In considering the utility of conjugated polymers, it is evident that the ability to process from aqueous solution provides a number of positive attributes, such as environmentally conscious processing methods, applications to biological systems, and control of ionic properties and interactions that are not possible with typical organic-solvent-compatible compositions. It is in this context that the field of conjugated polyelectrolytes (CPEs) was conceived and developed. This review presents synthetic developments in CPEs that have led to materials with unique optoelectronic properties, and illustrates how these properties have led to a range of applications in which the CPEs play a special role. We have selected examples and references that are illustrative of many concepts, and therefore apologize in advance to any whose specific examples may have been left out. The reader is encouraged to consult other authoritative reviews for different perspectives on the field.<sup>[3–11]</sup>

## From the Contents

1. Introduction	4301
2. Evolution and Synthesis of Conjugated Polyelectrolytes	4301
3. Photophysical Properties of Conjugated Polyelectrolytes: Effects of Polymer Aggregation and Self-Assembly	4306
4. Amplified Fluorescence Quenching in Conjugated Polyelectrolytes	4308
5. Application of Conjugated Polyelectrolytes as Sensor Materials	4310
6. Applications of Conjugated Polyelectrolytes in Optoelectronic Devices	4311
7. Summary and Outlook	4315

## 2. Evolution and Synthesis of Conjugated Polyelectrolytes

Research on conjugated polyelectrolytes was initiated in 1987 by Wudl, Heeger and co-workers, who reported water-soluble conducting polymers of 3-(2-sulfonatoethyl)-substituted (**1a**) and 3-(4-sulfonatobutyl)-substituted (**1b**) polythiophene (Scheme 1).<sup>[12]</sup> Both doped and undoped forms were prepared by electropolymerizing the corresponding



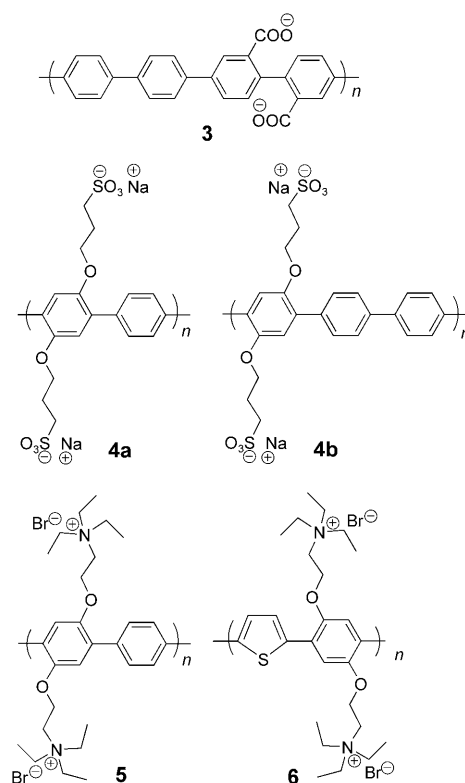
Scheme 1.

[\*] Dr. H. Jiang, Dr. P. Taranekekar, Prof. Dr. J. R. Reynolds, Prof. Dr. K. S. Schanze  
Department of Chemistry, University of Florida  
P.O. Box 117200, Gainesville, FL 32611-7200  
Fax: (+1) 352-392-9741 and (+1) 352-846-0296  
E-mail: reynolds@chem.ufl.edu  
kschanze@chem.ufl.edu  
Homepage: <http://www.chem.ufl.edu/~reynolds>  
<http://www.chem.ufl.edu/~kschanze>

methyl sulfonate monomers followed by conversion into the sodium salts. The conjugate acids of these polymers lose a proton upon oxidation with concomitant electron loss to produce self-doped polymers. This concept was demonstrated in parallel by Pomerantz, Reynolds and co-workers for *N*-propoxysulfonate derivatives of polypyrrole,<sup>[13,14]</sup> by which the self-doping concept was examined using quartz-crystal microgravimetry, and aqueous solutions could be cast to form electroactive films.

Dioxythiophene polymers were subsequently developed over the years owing to the enhancement of a number of properties (lower oxidation potential, reduced band gap, and stability of the doped and conducting form) and these polymers provided an excellent substrate upon which to develop new CPEs. For example, Chevrot and co-workers<sup>[15]</sup> and our group<sup>[16]</sup> synthesized a water-soluble poly(4-(2,3-dihydrothieno[3,4-*b*][1,4]dioxin-2-yl-methoxy)-1-butanefulfonic acid (PEDOT-S; **2**; Scheme 1) by chemical and electrochemical polymerization of the sulfonated monomers. The phenomenon of “acid doping” in aqueous and organic media was investigated spectroscopically and found to result in a reversible color change accompanied by relatively small changes in conductivity between oxidized and neutral films deposited on glass. An important observation was that thin films of PEDOT-S/poly(allylamine hydrochloride) in layer-by-layer (LbL) form has comparable properties to spin-coated PEDOT:PSS as a hole-injecting layer in near-IR-emitting PLEDs.<sup>[16]</sup>

In 1991, poly(*para*-phenylene) (PPP) rigid-rod CPEs were targeted. Novak and Wallow reported the first synthesis of poly(*p*-quaterphenylene-2,2'-dicarboxylic acid) (**3**; Scheme 2) using Suzuki cross-coupling of boronic acids and aryl halides.<sup>[17]</sup> The polymer, which has free acid groups, was completely insoluble in all common organic solvents, but was



Scheme 2.

soluble in dilute aqueous hydroxide solution, indicating the utility of converting these rigid polymers into true CPEs. The authors also observed that addition of divalent magnesium or zinc salts causes immediate precipitation to yield solvent- and water-resistant insoluble films.



Hui Jiang was born in China. After finishing his M.Sc. in physical chemistry and catalysis at Dalian Institute of Chemical Physics, Chinese Academy of Sciences, he joined Boston University, and completed his Ph.D. in 2005 under the direction of Dr. Guilford Jones II in the fields of photo-, physical, and analytic chemistry. He is currently a postdoctoral fellow with Dr. Kirk S. Schanze at the University of Florida, and is working with conjugated polymers and polyelectrolytes.



Prasad Taraneekar was born in India in 1975. After completing his M.S. in Applied Chemistry from the Institute of Chemical Sciences at Devi Ahilya University, he joined the University of Houston, USA, where he finished his Ph.D. on conducting polymers in 2006 under the supervision of Dr. R.C. Advincula. He is currently working as a postdoctoral fellow with Dr. J. R. Reynolds at the University of Florida, and is investigating linear and conjugated hyperbranched polyelectrolytes.



John R. Reynolds is a V.T. and Louise Jackson Professor of Chemistry at the University of Florida and an Associate Director of the Center for Macromolecular Science and Engineering. His research interests include electrically conducting and electroactive conjugated polymers, with work focused on the development of new polymers by manipulating their optoelectronic and redox properties.



Kirk S. Schanze is Professor of Chemistry at the University of Florida. His research is focused on the photophysics of organic and organometallic conjugated polymers and oligomers. His group also investigates applications of photoactive materials, including light-emitting diodes, fluorescent chemo- and biosensors, luminescence imaging, and solar cells. He has served as Editor-in-Chief of ACS Applied Materials & Interfaces since 2008.



PPP polymers have a remarkable thermal and chemical stability, which allows reactions on the polymer substituents to be carried out on preformed polymers without degradation of the main chain.<sup>[18]</sup> This has led to the utilization of the soluble-precursor method, in which a polymer that is soluble in organic solvents is synthesized and then purified and characterized by well-known techniques used in organic polymer chemistry. Using this approach, a neutral PPP polymer precursor is first obtained that contains reactive side groups, which were subsequently modified to ionic groups. For example, water-soluble CPEs were obtained by substituting ester side groups on the PPP backbone and subsequently cleaving the ester groups to generate acid groups **3** (Scheme 2). The ester cleavage was performed by base hydrolysis or using thermally cleavable ester groups to generate water-soluble PPP polyelectrolytes.<sup>[19–21]</sup>

The first report on sulfonated PPPs in 1994 by Wegner and co-workers<sup>[22]</sup> was quickly followed in the same year by our group<sup>[23]</sup> on “self-doped” poly[2,5-bis(3-sulfonatopropoxy)-1,4-phenylene-*alt*-1,4-phenylene] **4a** (Scheme 2). This polymer features pendant sulfonate groups, which not only impart water solubility but also serve as the charge-compensating dopant ion during redox switching. In 1998, we<sup>[24]</sup> extended our work on sulfonated PPPs and performed a detailed investigation using poly[2,5-bis(3-sulfonatopropoxy)-1,4-phenylene-*alt*-4,4'-biphenylene] sodium salt **4b**. The pH dependence of the polymerization reaction was investigated, and polyelectrolyte LbL films of **4b** were fabricated with poly(ethylene-imine) (PEI) using LbL self-assembly and incorporated into blue-electroluminescent devices.

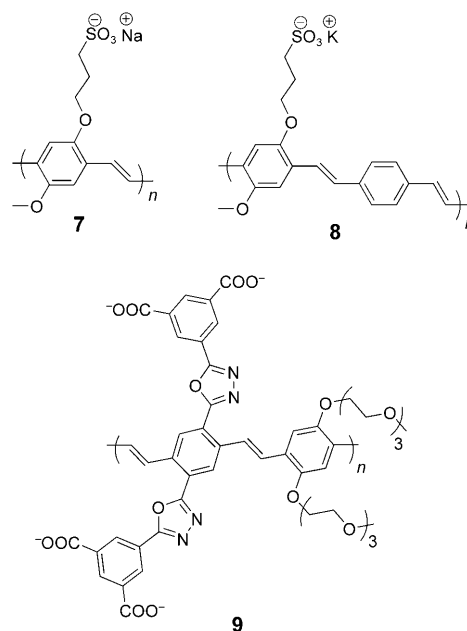
The first cationic PPP CPEs based on homopolymers and copolymers were synthesized using the soluble-precursor route by initial polymerization of a neutral PPP substituted with side chains terminated with primary alkyl halides. Quaternization of the alkyl halides in nearly quantitative yields were achieved using trialkyl amines.<sup>[25]</sup> In a subsequent report, Wittemann and Rehahn described the synthesis of a cationic PPP, which contains multiple charges on each repeat unit, using tetramethylethylenediamine (TMEDA) to provide good solubility in water and even polar organic solvents.<sup>[26]</sup>

In 2000, we reported a fluorescence study of the PPP polycation **5** (Scheme 2) prepared by a neutral soluble precursor featuring side chains functionalized with tertiary amine groups. Polycation **5** was subsequently prepared by quaternization of the tertiary amine units with ethyl bromide.<sup>[27]</sup> This polyelectrolyte was used in solution and as thin films to demonstrate the amplified fluorescence-quenching effect. This work was inspired by an early study by Swager and Zhou, who demonstrated amplified fluorescence quenching for the first time using neutral, organic-solvent-soluble fluorescent conjugated polymers bearing receptor sites for a target.<sup>[28]</sup>

In 2005, we reported the synthesis and photophysical properties of the cationic CPE **6** (Scheme 2), which features a backbone consisting of alternating phenylene and thienylene units.<sup>[29]</sup> CPE **6** was synthesized by a precursor approach in which a neutral copolymer that contains tertiary amine substituents was produced by a Stille coupling; the ammonium units were subsequently generated by quaternization with

ethyl bromide. The green fluorescence of the cationic CPE was efficiently quenched by anions such as  $[\text{Fe}(\text{CN})_6]^{4-}$  and anthraquinone-2,7-disulfonate (AQS).

An important class of CPEs that feature the poly(phenylenevinylene) (PPV) conjugated backbone was developed in 1990 by Wudl and Shi.<sup>[30]</sup> They reported the water-soluble polymer poly(5-methoxy-2-(3-sulfopropoxy)-1,4-phenylenevinylene) (MPS-PPV; **7**; Scheme 3) which was synthesized



Scheme 3.

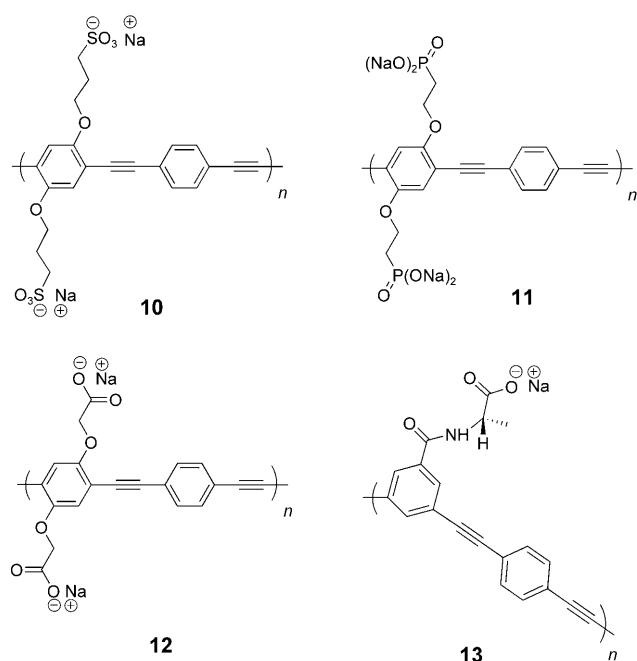
using a conventional precursor polymer approach with sulfonyl chloride groups that were hydrolyzed in DMF and water for conversion into a fully conjugated form. This work served as an excellent platform for several important investigations that demonstrate the use of conjugated polymers bearing ionic side groups for sensors based on fluorescence (see Section 4).<sup>[31]</sup>

In 2006, Shen and co-workers reported a facile chemical approach to enhance the photoluminescence of MPS-PPVs by synthesizing the anionic conjugated copolymer of poly[(2-methoxy-5-propyloxysulfonate)-1,4-phenylenevinylene]-*alt*-(1,4-phenylenevinylene)] (CO-MPSPPV; **8**) by alternately incorporating the rigid *p*-phenylenevinylene unit into the conjugated backbone.<sup>[32]</sup> In 1999, another group of researchers designed a PPV-type CPE **9** bearing cross-conjugated side chains with carboxylate groups (Scheme 3).<sup>[33]</sup> This polymer was designed with the objective of producing a nanoporous polymer network with controllable uniform pore sizes by means of LbL self-assembly. The carboxylate groups provide the polymer with water solubility and interchain hydrogen bonds in the solid state, which act as anchors during deposition. Polymer **9** was obtained by a Heck reaction and is soluble in DMSO or dilute aqueous bases, but insoluble in common organic solvents.

Poly(phenylene-ethynylene) (PPE) CPEs have a versatile chemistry that make these materials one of the most studied

systems. They are also strongly fluorescent, making them amenable for applications such as light emission. The Sonogashira method is generally employed to produce high-molecular-weight PPEs by copolymerizing a dihalo arene and a diethynyl arene. PPEs can also be obtained from metathesis of diethynyl-substituted aromatic monomers; however, this approach has limited functional-group tolerance and has not been applied to CPE synthesis.<sup>[34,35]</sup> In 1997, Li and co-workers reported carboxylate-based, *meta*-linked PPEs for the first time in a one-pot synthesis by copolymerization of acetylene with 3,5-diodobenzoic acid.<sup>[36,37]</sup> Swager and co-workers have also carried out extensive work on the synthesis of a variety of PPEs for applications involving amplified quenching and pH sensors.<sup>[8,38]</sup>

In 2002, we reported the synthesis of sulfonated PPE-SO<sub>3</sub> **10** (Scheme 4), which was obtained by Sonogashira coupling with 1,4-diethynylbenzene in a DMF–water mixture and



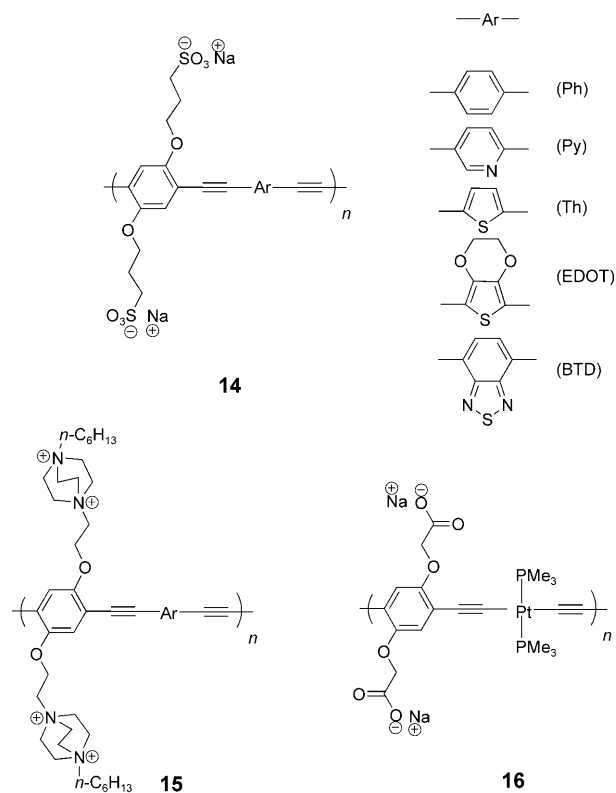
Scheme 4.

catalyzed by [Pd(PPh<sub>3</sub>)<sub>4</sub>]/CuI.<sup>[39]</sup> This polymer is strongly fluorescent, and its fluorescence is quenched very efficiently in an amplified quenching process.<sup>[40]</sup> A similar CPE (**11**) features phosphonate groups appended to the polymer backbone (Scheme 4). Using the neutral precursor polymer approach described earlier, the CPE substituted with phosphonate ester groups was prepared so that it is soluble in common organic solvents, enabling the material to be structurally characterized by NMR spectroscopy and gel permeation chromatography.<sup>[41]</sup> After hydrolysis of the phosphonate ester groups and subsequent base extraction with aqueous sodium hydroxide, water-soluble CPE **11** was obtained.

In 2006, we reported the conjugated polyelectrolyte PPE-CO<sub>2</sub> (**12**; Scheme 4) prepared by a precursor route. Sonogashira coupling was used to polymerize an equimolar mixture

of 2,5-bis(dodecyloxycarbonylmethoxy)-1,4-diiodobenzene and 1,4-diethynylbenzene. Using a dual polymer approach, CPE **12** was coadsorbed onto nanocrystalline TiO<sub>2</sub> with a carboxylated polythiophene to give rise to spectral broadening for photovoltaic applications.<sup>[42]</sup> In the same year, we reported a *meta*-linked PPE featuring optically active side groups based on L-alanine (*m*PPE-Ala, **13**). Sonogashira coupling reactions were used to prepare the precursor polymer functionalized with benzyl ester groups; the ester protecting groups could then be removed by mild basic hydrolysis, affording *m*PPE-Ala substituted with carboxylic acid groups.<sup>[43]</sup> Although these *para*- and *meta*-linked PPEs stand out as potential materials for fluorescence-based biosensors, we have investigated other interesting PPE-type CPE structures that show promising biological applications.<sup>[44–47]</sup>

In an attempt to understand the structure–property relationships of CPEs, we employed various synthetic methods to study the effects of energy-gradient-driven exciton and/or charge transfer on photoconversion efficiency and the effect of band-gap modulation. In 2006, a series of both cationic and anionic poly(arylene-ethynylene) (PAE) CPEs were prepared using Sonogashira coupling chemistry (Scheme 5).<sup>[48]</sup> The series consists of five pairs of polymers that share the same poly(arylene-ethynylene) backbone. One member of each pair contains anionic sulfonate side groups (**14**), whereas the other contains cationic bis(alkylammonium) side groups (**15**). The repeat-unit structure of the poly(arylene-ethynylene) backbone consists of a bis-(alkoxy)phenylene-1,4-ethynylene unit that alternates with a



Scheme 5.

second arylene-ethynylene moiety. The different arylene units induce variations in the HOMO–LUMO band gap across the series of polymers, resulting in a series of CPEs that are soluble in methanol and water and have controlled photo-physical properties.

In 2004, we developed a novel class of water-soluble, organometallic polymers formed of platinum alternating with phenylene-ethynylene units to produce the platinum(II) acetylide-based CPE **16** (Scheme 5).<sup>[49]</sup> A copper-catalyzed step-growth polymerization was carried out using  $[\text{PtCl}_2(\text{PMe}_3)_2]$  and 2,5-bis(dodecyloxycarbonylmethoxy)-1,4-diethynylbenzene to form a precursor polymer in which the carboxyl groups were protected as dodecyl esters. The progress of the polymerization reaction was followed by gel permeation chromatography, and the reaction was discontinued once the molecular weight no longer increased. The hydrolysis of the dodecyl-terminated precursor polymer was performed using aqueous  $n\text{Bu}_4\text{NOH}$  to yield CPE **16**. Luminescence experiments showed that **16** is phosphorescent at room temperature.<sup>[49]</sup>

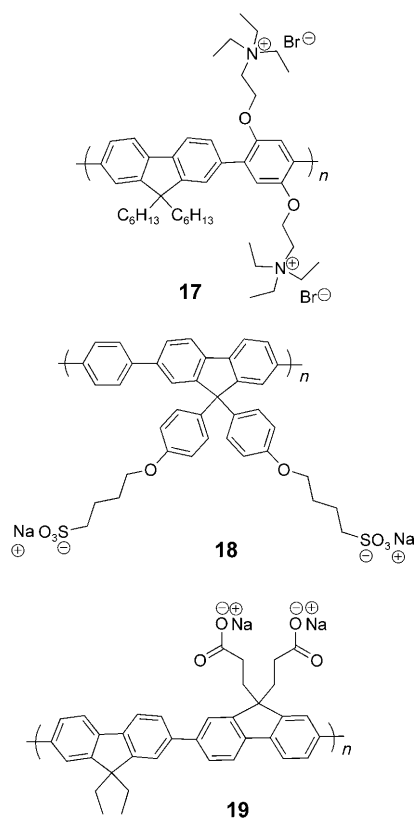
Polyfluorene (PF) CPEs are yet another interesting class of materials that have recently received considerable attention. In 2002, Huang and co-workers introduced PF CPEs in which a cationic, water-soluble blue-emitting CPE with a backbone consisting of alternating fluorene and phenylene units (**17**; Scheme 6) was prepared through a facile post-polymerization approach.<sup>[50]</sup> In addition to a full structural characterization, this approach allowed control of the extent

of ionization based on quaternization of the amino side groups. The neutral amino-substituted polymer could be made water soluble upon addition of a few drops of acetic acid. Bazan and co-workers have also reported cationic polyfluorene and fluorene-containing copolymers that were synthesized by Suzuki polymerization, yielding the precursor polymer with  $-\text{NMe}_2$  groups that were subsequently quaternized. Salt-exchange reactions were carried out to investigate the effect of counterions in devices.<sup>[9,51]</sup> Similarly, in 2004, Cao et al. demonstrated the use of PF-CPEs using environmentally friendly solvents, such as alcohols, in the fabrication of devices.<sup>[52]</sup>

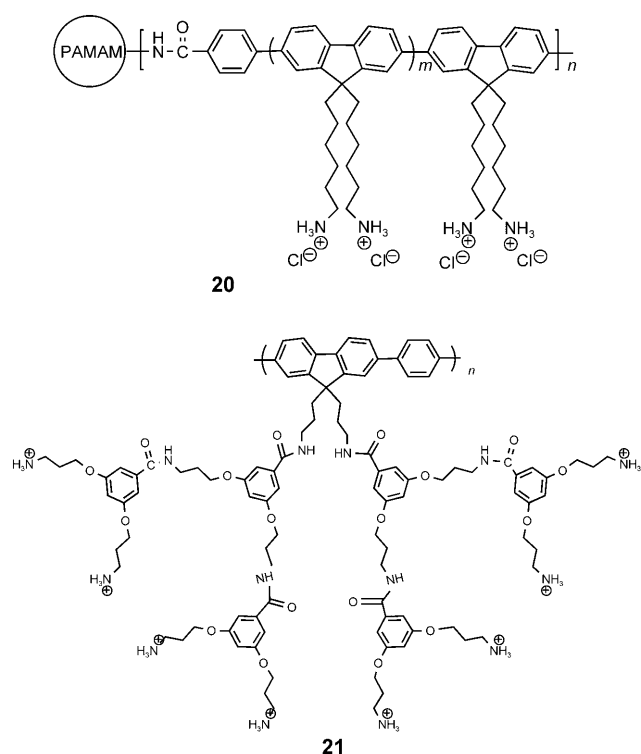
There are numerous reasons to develop CPEs and tailor their phase behavior, structure, and supramolecular form in water. In particular, attention was paid to the solubilization and self-organization characteristics of a water–polyfluorene–surfactant (amphiphile) system composed of polyelectrolyte (PBS-PFP) **18** (Scheme 6).<sup>[53,54]</sup> The anionic hairy-rod PF copolymer was prepared by a palladium-catalyzed Suzuki coupling of a mixture of 2,7-dibromo-9,9-bis(4-sulfonylbutoxy)fluorene and 1,4-phenylenediboric acid using a 5:1 toluene/butanol mixture.

More recently, we reported fluorene copolymer CPE **19** that is functionalized with carboxylic acid groups (Scheme 6).<sup>[55]</sup> Previous work on Suzuki coupling for small-molecule synthesis illustrated the activation of boronic acids by fluoride salts, such as cesium fluoride and tetrabutylammonium fluoride.<sup>[56]</sup> In our work, we demonstrated the optimization of the base-free Suzuki polymerization under a variety of conditions with cesium fluoride and tetrabutylammonium fluoride (TBAF) used as fluoride sources to initially generate a neutral precursor polymer. The precursor polymer obtained using the dibromide and diboronate ester of fluorene monomers was subsequently hydrolyzed to generate the carboxylic acid groups of **19**. Using DMAC and DME as solvents, high-yield polymerizations were obtained with cesium fluoride, with DME as solvent giving a notably larger number-average molecular weight.

The synthetic design of PF-CPEs have also focused on either having dendritic side groups or peripheral modification of dendrimers. In 2005, Bazan and co-workers synthesized four generations of phenylene-fluorene- and phenylene(bis-fluorene)-terminated polyamidoamine (PAMAM) dendrimers by coupling activated esters with commercially available PAMAM precursors.<sup>[57]</sup> The treatment of Boc-terminated pendant groups on the photoactive units with 3M HCl in dioxane yields cationic water-soluble dendrimers **20** (Scheme 7). In 2007, Bo and co-workers reported a set of water-soluble dendronized polyfluorenes bearing peripheral ammonium groups.<sup>[58]</sup> These materials were synthesized in two steps, namely Suzuki polycondensation of dendritic macromonomers carrying peripheral Boc-protected amino groups with 1,4-benzenediboric acid propane–diol ester followed by deprotection of the resulting Boc-protected dendronized polymers with aqueous HCl. All of the protected dendronized polyfluorenes showed good solubility in common organic solvents such as THF and dichloromethane. After deprotection, the zero-generation polymers were only partially soluble in water, but the polymers having first- and



Scheme 6.



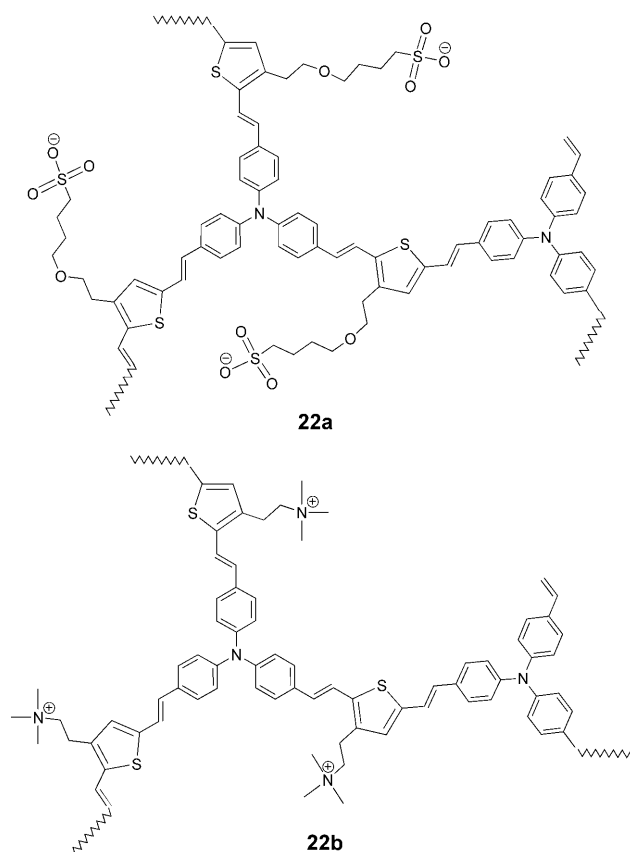
Scheme 7.

second-generation dendrimers (**21**, Scheme 7) were fully soluble in water.

To date, no work on ionic conjugated dendrimers has been reported. However in 2007, we reported a dendrimer-like but randomly branched conjugated hyperbranched polyelectrolyte (HB-CPE).<sup>[59]</sup> In that work, we prepared complementary pairs of polymers that feature the same conjugated backbone, but contain either anionic or cationic side groups. We described a direct synthetic approach in which a B<sub>2</sub>-type thiophene monomer substituted with either quaternized amino or sulfonate pendant groups is reacted with an A<sub>3</sub>-type tris(4-vinylphenyl)amine monomer. The synthesis of hyperbranched conjugated polymers being either anionically charged with sulfonate groups (**22a**) or cationically charged with quaternized amine groups (**22b**; Scheme 8) were performed using the A<sub>3</sub> + B<sub>2</sub> type approach based on Heck polycondensation. These polymers were used to construct CPE bilayers on nanostructured TiO<sub>2</sub>, affording relatively efficient photoelectrochemical cells (see Section 6.2).

### 3. Photophysical Properties of Conjugated Polyelectrolytes: Effects of Polymer Aggregation and Self-Assembly

The photophysical properties of CPEs have been extensively investigated, both from the fundamental viewpoint and with respect to applications in chemo- and biosensors and organic optoelectronic devices. In general, their optical properties are determined by the chemical and electronic structure of the conjugated backbone. Therefore, similar



Scheme 8.

absorption and photoluminescence spectra are usually observed for conjugated polymers and polyelectrolytes with the same backbone structure and different side groups. However, owing to their inherently amphiphilic structures (hydrophobic backbone and hydrophilic side groups), CPEs have a tendency to aggregate in aqueous solution or polar organic solvents, and as a result their photophysical properties can be strongly dependent on the solvent.

To illustrate some of these features, the series of poly(arylene-ethynylene) CPEs (Scheme 5) can be considered, which were the subject of a comprehensive study reported in 2006.<sup>[48]</sup> This series of CPEs consists of five pairs of polymers that share the same poly(arylene-ethynylene) backbone substituted with either anionic (**14**, PPE-Ar-SO<sub>3</sub><sup>-</sup>) or cationic (**15**, PPE-Ar-(4<sup>+</sup>)) side groups. Absorption and fluorescence spectroscopy shows that the optical properties of each pair of anionic and cationic CPEs that share the same backbone structure are virtually the same. The different arylene units used in the conjugated backbone induce significant variation in the band gap across the series, so that the absorption maxima range from 400 to 550 nm and the fluorescence maxima range from 440 to 600 nm (Figure 1).<sup>[48]</sup>

We have also carried out a broad set of studies to explore how CPE aggregation influences the photophysical properties of the materials. These studies demonstrate that under specific solution conditions, the CPEs aggregate and the aggregation process induces significant changes in both absorption and fluorescence spectra.<sup>[39–41,60]</sup> In general, poly-



**Figure 1.** Fluorescence of methanol solutions of PPE-Ar-SO<sub>3</sub><sup>−</sup> (**14**) under illumination with near-UV light. From left to right: Ph, Py, Th, EDOT and BTB. (From Ref. [48].)

(arylene-ethynylene) CPEs with anionic side groups, such as sulfonate (−SO<sub>3</sub><sup>−</sup>) or carboxylate (−CO<sub>2</sub><sup>−</sup>), exist as molecularly dissolved chains in methanol; however, they exist as aggregates if either water<sup>[39,40]</sup> or a divalent cation, such as calcium(II),<sup>[60]</sup> is added to the methanol solvent. CPEs substituted with weakly ionized polyelectrolyte groups, such as phosphonate (−PO<sub>3</sub><sup>2−</sup>), aggregate in water at neutral pH; however, the aggregates disperse when the pH increases above 8.<sup>[41]</sup> The effects of other factors on CPE chain aggregation, such as concentration, temperature, solution ionic strength, and added surfactant, have also been investigated by other researchers.<sup>[61]</sup>

A particularly clear example of the effect of aggregation on the optical properties of a CPE is seen by comparing the absorption and fluorescence spectra of PPE-SO<sub>3</sub><sup>−</sup> (**10**; Scheme 4) in water, methanol, and a 1:1 water/methanol mixture (see Figure 2). As the amount of water in the solvent increases, the absorption and emission of PPE-SO<sub>3</sub><sup>−</sup> undergo a red-shift. The effect is most pronounced in the fluorescence of the polymer. In methanol, in which the polymer exists as molecularly dissolved (non-interacting) chains, the fluorescence appears as a sharp, structured, and narrow band that has a very small Stokes shift relative to the absorption band. However in water, in which the polymer is strongly aggregated, the fluorescence appears as a broad, structureless band

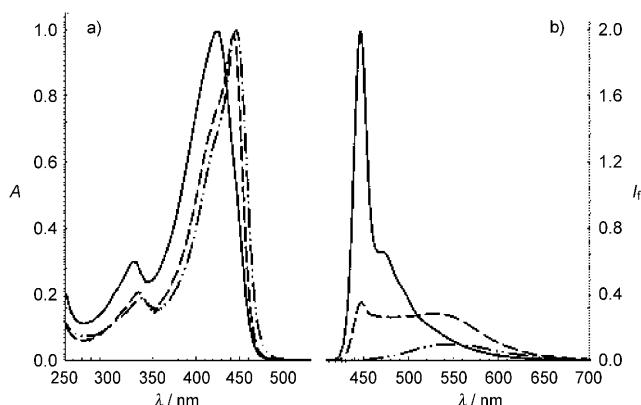


**Figure 2.** Absorption (left) and fluorescence (right) spectra of PPE-SO<sub>3</sub><sup>−</sup> in CH<sub>3</sub>OH (—), 1:1 CH<sub>3</sub>OH/H<sub>2</sub>O (---), and H<sub>2</sub>O (·····). Fluorescence spectra are normalized to reflect relative quantum yields. (From Ref. [40].)

that is red-shifted significantly from its position in methanol.<sup>[39,40]</sup>

Aggregation of a CPE in a good solvent such as methanol can be induced by addition of polyvalent metal cations. For example, when calcium(II) ions are added to a methanol solution of PPE-CO<sub>2</sub><sup>−</sup> (**12** in Scheme 4), spectral changes are observed (Figure 3) that are similar to those seen when PPE-SO<sub>3</sub><sup>−</sup> is aggregated in aqueous solution (compare with Figure 2).<sup>[60,62]</sup> As Ca<sup>2+</sup> is a closed-shell cation and cannot

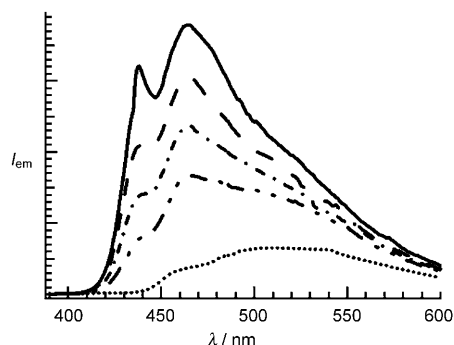


**Figure 3.** Emission spectra of 10 μM PPE-CO<sub>2</sub><sup>−</sup> (structure **12** in Scheme 4) in the presence of 0 μM (—), 2.5 μM (---), 5.0 μM (— · —), 7.5 μM (— · — · —), and 10.0 μM (·····) of Ca<sup>2+</sup> ions in methanol. (From Ref. [60].)

act as an acceptor of electrons or energy, the observed fluorescence quenching and red-shift are due to CPE chain aggregation. Calcium(II) ions effectively cross-link PPE-CO<sub>2</sub><sup>−</sup> chains by complexing with the carboxyl side groups of the polymer. This conclusion is further supported by the stoichiometry of the complex formation, which shows that the effect of calcium(II) ions on the optical properties saturates when the ratio of calcium(II) ions to polymer repeat units is 1:1.

In a separate series of studies, we have shown that the primary structure (connectivity) of the CPE backbone can induce the polymer to self-assemble into a helical secondary structure in water. In particular, absorption and fluorescence spectra (Figure 4) of the *meta*-linked CPE, *m*-PPE-SO<sub>3</sub><sup>−</sup>, in methanol, water, and in mixtures of the two solvents are consistent with the notion that the polymer exists in a random-coil conformation in methanol (good solvent) and in a helical conformation in water (poor solvent).<sup>[63]</sup> The conclusion that *m*-PPE-SO<sub>3</sub><sup>−</sup> exists in a helical conformation in water is supported by the fact that the spectral changes seen when the solvent is changed from methanol to water are virtually identical to those observed by Moore and co-workers for a series of *meta*-linked phenylene-ethynylene oligomers when the solvent is varied from good (chloroform) to poor (acetonitrile).<sup>[64–66]</sup>

More direct evidence that the differences in absorption and fluorescence spectra arise when the solvent for *m*-PPE-SO<sub>3</sub><sup>−</sup> is changed from methanol to water because of polymer folding into a helical conformation come from circular dichroism studies of the structurally related CPE *m*PPE-Ala (**13**; Scheme 4).<sup>[43]</sup> This polymer has the same backbone



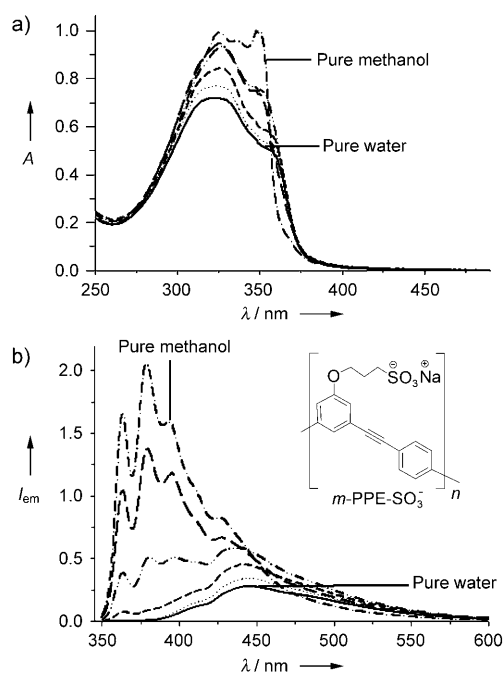


**Figure 4.** Absorption (a) and fluorescence (b) spectra of *m*-PPE-SO<sub>3</sub><sup>-</sup> in methanol, water, and methanol/water mixtures. (From Ref. [63].)

structure as *m*-PPE-SO<sub>3</sub><sup>-</sup>, but it features optically active side groups based on L-alanine. As shown in Figure 5, *m*PPE-Ala exhibits a strong bisignate circular dichroism spectrum in the

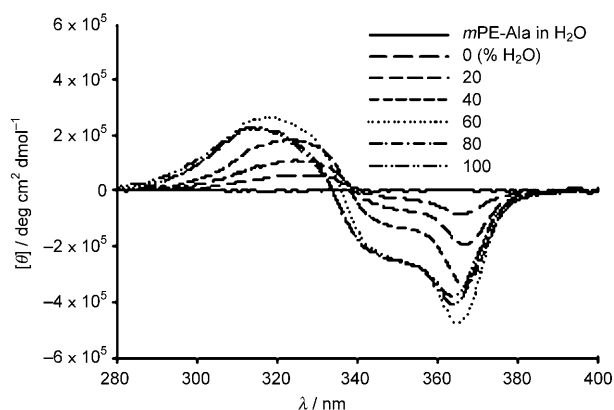
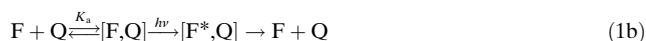


**Figure 5.** CD spectra of the model compound *m*PPE-Ala in water (solid black line) and *m*PPE-Ala in methanol, water, and methanol/water mixtures. (From Ref. [43].)

region corresponding to the  $\pi$ - $\pi^*$  absorption of the polymer backbone in methanol, water, or mixtures of the two solvents. The bisignate circular dichroism signal observed for *m*PPE-Ala arises because the conjugated backbone is in a chiral environment produced by the helical conformation, and the chiral center present in the optically active side groups induces the polymer to fold preferentially into the *M*-conformation.

#### 4. Amplified Fluorescence Quenching in Conjugated Polyelectrolytes

Much of the interest concerning properties and applications of CPEs is associated with the observation of efficient fluorescence quenching at low quencher concentration; that is, “amplified quenching” or “superquenching”.<sup>[31,67]</sup> Before discussing this phenomenon, it is necessary to briefly review the standard mechanisms used to explain fluorescence quenching.<sup>[68]</sup> Fluorescence quenching can occur by two limiting mechanisms, namely dynamic [Eq. (1a)] and static [Eq. (1b)]. In Equations (1a) and (1b), F\* is an excited-state chromophore, Q is a quencher,  $k_q$  is the bimolecular quenching rate constant, and  $K_a$  is the association constant for formation of the ground-state complex [F,Q]. Treatment of fluorescence-intensity quenching data with the standard Stern–Volmer method yields Equation (2), where  $I_0$  and  $I$  are the fluorescence intensities in the absence and presence of Q, respectively, and  $K_{SV}$  is the Stern–Volmer quenching constant. If quenching is dominated by the dynamic pathway [Eq. (1a)],  $K_{SV} = k_q \tau_0$ , where  $\tau_0$  is the fluorescence lifetime of F\* without Q; whereas in the limit for which static quenching dominates,  $K_{SV} = K_a$ . In either case, according to Equation (2) the Stern–Volmer plot of  $I_0/I$  versus [Q] is expected to be linear. However, in many situations with quencher–CPE systems, the Stern–Volmer plots are curved upward (i.e., superlinear). This can arise from a variety of processes, such as mixed static and dynamic quenching, variation in the association constant with quencher concentration, and chromophore (or polymer) aggregation.



$$I_0/I = 1 + K_{SV}[Q] \quad (2)$$

The concept of amplified quenching, or the molecular wire effect associated with conjugated polymers, was first described by Swager and Zhou in 1995.<sup>[67]</sup> They reported the preparation and photophysical characterization of a series of neutral PPEs of variable molecular weight that are soluble in organic solvents and that contain a cyclophane receptor on each repeat unit. The most interesting aspect of this work comes from their study of the fluorescence quenching of the polymer by the electron acceptor *N,N'*-dimethyl-4,4'-bipyridinium (methylviologen, MV<sup>2+</sup>). This quencher was selected because it is known to associate with the cyclophane receptors that are attached to every repeat unit. Compared with the quenching effect for a monomeric model compound, the polymers show considerably larger quenching effect (a maximum increase in  $K_{SV}$  by a factor of 66), suggesting that the quenching response is amplified in the polymers relative to the monomeric model compound. Furthermore, the amplification factor, defined as the ratio of  $K_{SV}$  for the polymer divided by  $K_{SV}$  for the model compound, increases with polymer chain length, suggesting that the effect is related to the ability of the fluorescent exciton to migrate along the polymer chain.

The amplified quenching efficiency of the conjugated polymer is attributed to the molecular-wire effect; that is, excitation delocalization and transport by the polymer chain (Figure 6).<sup>[67]</sup> Upon absorption of light, a singlet exciton (a

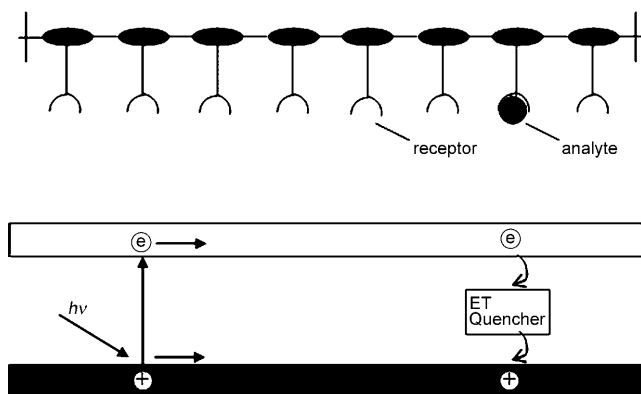


**Figure 6.** “Molecular wire” effect in conjugated polymers with receptors. (From Ref. [67].)

bound electron–hole pair) is generated at an arbitrary position on the polymer backbone. The conjugated polymer acts as a conduit for the exciton, allowing it to migrate very rapidly along the chain. When the exciton reaches a repeat unit that contains a quencher-occupied receptor (i.e., a trap site), it is quenched. Because of the extremely efficient exciton migration along the conjugated polymer chain, a single quencher molecule bound to one receptor site can quench many repeat units in the polymer chain, leading to the amplified quenching response of the polymer to the target analyte.

The amplified quenching effect in CPEs was first observed by Whitten and co-workers in the course of an investigation of the fluorescence quenching of MPS-PPV (**7**; Scheme 3) by  $MV^{2+}$ .<sup>[31]</sup> Specifically, addition of 100 nM of  $MV^{2+}$  to an aqueous solution of the polymer ( $c \approx 10^{-5}$  M in polymer repeat units) affords extraordinarily efficient quenching of the polymer fluorescence, coupled with a distinct red-shift in the absorption spectrum (Figure 7). For low concentrations of  $MV^{2+}$  (0–0.5  $\mu$ M), the Stern–Volmer plot for fluorescence

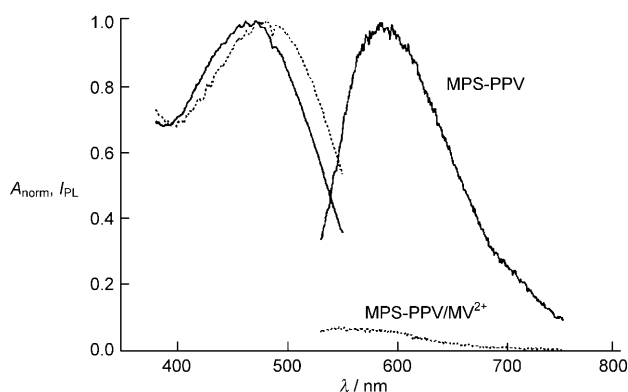


**Figure 7.** Absorption (left) and fluorescence (right) spectra of MPS-PPV in water with (solid line) and without (dotted line) 100 nM  $MV^{2+}$ . (From Ref. [31].)

quenching is linear with  $K_{SV} = 1.7 \times 10^7 \text{ M}^{-1}$ . This extremely large  $K_{SV}$  value indicates that the predominant quenching mechanism is static quenching and involves an ion-pair complex between the anionic MPS-PPV chains and the cationic quencher  $MV^{2+}$ . In addition, other processes are also believed to be involved, including rapid and efficient exciton diffusion within the polymer chains, and quencher-induced aggregation of the polymer chains, which enhances the efficiency of intrachain excimer formation and interchain exciton hopping.<sup>[31]</sup>

We have been studying the mechanism and dynamics of amplified quenching in poly(phenylene-ethynylene) CPEs. As one example, we investigated the fluorescence quenching of PPE- $\text{SO}_3$  (**10**; Scheme 4) by a series of cationic cyanine dyes that bind to the polymer by electrostatic and solvophobic interactions.<sup>[40,69]</sup> The dyes quench the polymer fluorescence by energy transfer, and the dynamics can be monitored either by the decay of the polymer fluorescence (the energy donor) or the rise of the dye fluorescence (the energy acceptor). This study showed that the rate of fluorescence quenching of PPE- $\text{SO}_3$  by a red-emitting cyanine dye (HMDC) is remarkably fast, with a significant component of the energy transfer taking place on a timescale of less than 1 ps. A model was developed based on a random walk of the exciton within the polymer chain combined with long-range direct energy transfer (Förster transfer) between the polymer and the dye quencher. Comparison of the predictions of this model with the experimental dynamics data reveals that rapid migration of the singlet exciton to dye–complex sites is mainly responsible for the ultrafast energy transfer; contributions to the quenching by direct, long-range resonance energy transfer are negligible. The work also clearly demonstrated that the amplified quenching effect is enhanced when PPE- $\text{SO}_3$  is aggregated, presumably as the exciton is transported between polymer chains in the aggregate.

As discussed in Section 3, calcium(II) ions induce aggregation of PPE- $\text{CO}_2^-$  in methanol solution in a controlled manner (Figure 3).<sup>[60,62]</sup> More importantly, this induced polymer aggregation has a significant effect on the efficiency of fluorescence quenching by  $MV^{2+}$ . In particular, the fluorescence quenching response to  $MV^{2+}$  increases with increasing calcium(II) ion concentration (Figure 8), and the onset of upward curvature (superlinear effect) in the Stern–Volmer plot shifts to lower quencher concentrations. In a methanol

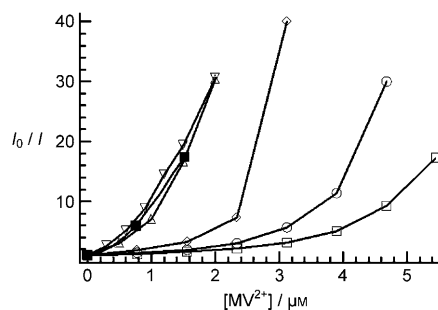


**Figure 8.** Quenching of PPE- $\text{CO}_2^-$  emission by  $MV^{2+}$  in water (■) and in methanol with 0  $\mu$ M (□), 2.5  $\mu$ M (○), 5.0  $\mu$ M (◇), 7.5  $\mu$ M (△), or 10.0  $\mu$ M (▽)  $\text{Ca}^{2+}$ . (From Ref. [60].)

solution containing more than  $7.5\ \mu\text{M}$   $\text{Ca}^{2+}$  ions, the Stern–Volmer response is similar to that observed in aqueous solution, in which  $\text{PPE-CO}_2^-$  exists as aggregates. These results provide unambiguous evidence that quencher-induced polymer aggregation is responsible for the superlinear Stern–Volmer response that is typically observed when conjugated polyelectrolytes are quenched by multivalent ions.

In summary, the study of amplified quenching in CPE-quencher systems reveals the following important features. First, there are two key elements that give rise to the process: ion-pairing between a CPE chain and an oppositely charged quencher ion, and rapid diffusion of singlet excitons within single CPE chains. Furthermore, fluorescence quenching is further enhanced under conditions under which the CPE chains are strongly aggregated.

### 5. Application of Conjugated Polyelectrolytes as Sensor Materials

A motivation for the extensive research in conjugated polymers and CPEs lies in their potential development as materials for chemo- and biosensors. The concept of amplified quenching in fluorescent conjugated polymers, first demonstrated by Swager and Zhou,<sup>[67]</sup> and the realization of this concept in water soluble CPEs by Whitten and co-workers<sup>[31]</sup> paved the way for further development of this important class of conjugated polymers as novel sensory materials. Over the past several years, the use of CPEs as sensory materials, with emphasis on biosensing, has been the subject of considerable research interest. Various specific interactions have been explored, such as biotin–avidin<sup>[5]</sup> and antigen–antibody<sup>[70]</sup> interactions, and non-specific interactions, such as electrostatic and hydrophobic binding. Relevant targets include polynucleic acids,<sup>[71]</sup> proteins,<sup>[72]</sup> enzymes,<sup>[73–77]</sup> carbohydrates<sup>[78]</sup> and small molecules, and metal ions. Detection of enzyme kinetics and/or protein conformational changes has been of particular interest. Recently, both Whitten and Swager have authored review articles on this topic,<sup>[8,10]</sup> and here we will only focus on the work done in our laboratories to illustrate specific sensor design principles.<sup>[44,46,47,79]</sup>

CPE-based fluorescent sensors can operate either in the “turn-off” or “turn-on” modes. In the turn-off mode, the polymer is fluorescent in the absence of the analyte, and upon addition of the analyte the polymer fluorescence is turned off by a specific (amplified) quenching mechanism. By contrast, for the turn-on approach, the fluorescence response of the sensor system is reversed; i.e., addition of the analyte induces an increase of the polymer fluorescence. The turn-off and turn-on responses can be realized by many different processes, including simple redistribution of quencher ions between polymer and analyte,<sup>[46,79]</sup> target-induced modification of the quencher structure,<sup>[45,80]</sup> and/or of the physical state (aggregation and conformation) of the polymer.<sup>[44,81]</sup>

Recently, a fluorescence turn-on sensor with high selectivity for pyrophosphate (PPi) was developed.<sup>[79]</sup> This sensor is based on reversible quenching in the system consisting of  $\text{PPE-CO}_2^-$  (**12**; Scheme 4),  $\text{Cu}^{2+}$  (quencher) and PPi. Addi-

tion of  $\text{Cu}^{2+}$  ions to  $\text{PPE-CO}_2^-$  leads to efficient quenching ( $K_{\text{SV}} \approx 10^6\ \text{M}^{-1}$ ); a solution containing  $10\ \mu\text{M}$  polymer and  $10\ \mu\text{M}$   $\text{Cu}^{2+}$  is nearly non-fluorescent. However, upon addition of PPi to the quenched solution containing  $\text{PPE-CO}_2^-$  and  $\text{Cu}^{2+}$ , the polymer fluorescence is recovered, enabling a turn-on sensor for pyrophosphate (Figure 9), with a detection limit for PPi of 80 nM. Fluorescence recovery arises because PPi binds strongly to  $\text{Cu}^{2+}$ , effectively acting as a sequestering agent and disrupting the metal ion/polymer complex.

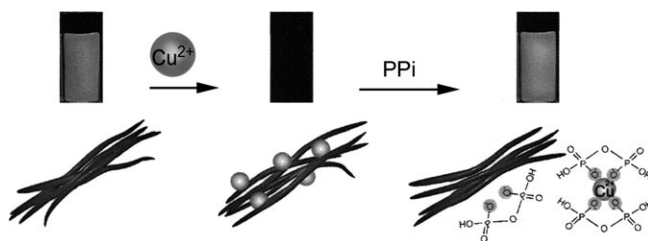


**Figure 9.**  $\text{PPE-CO}_2^-$  fluorescence quenching by  $\text{Cu}^{2+}$  ions, and recovery in the presence of pyrophosphate (PPi). (From Ref. [79].)

Analyte-induced modification of quencher structure is another approach that has been utilized to construct CPE-based fluorescent sensors. As one example of this approach, we developed a sensor for carbohydrates by using  $\text{PPE-SO}_3$  (**10**; Scheme 4) and a cationic quencher comprising a bisboronic acid functionalized benzyl viologen ( $p\text{-BV}^{2+}$ ).<sup>[80]</sup> Not surprisingly, the fluorescence of  $\text{PPE-SO}_3$  is efficiently quenched by  $p\text{-BV}^{2+}$  (off-state), as this species is an analogue of  $\text{MV}^{2+}$ , and quenches the polymer's fluorescence by a charge-transfer mechanism. At neutral pH, addition of glucose or fructose to a solution of  $\text{PPE-SO}_3$  and  $p\text{-BV}^{2+}$  leads to efficient recovery of the fluorescence from the polymer. Fluorescence recovery occurs because a complex forms between the vicinal alcohol units in the carbohydrate and the boronic acid functional groups in  $p\text{-BV}^{2+}$  (Figure 10a). The resulting carbohydrate–boronate ester moiety is anionic and therefore neutralizes the cationic charge on the viologen moiety, disrupting the electrostatic binding between the quencher and  $\text{PPE-SO}_3$  (on-state, Figure 10b). The sensor system shows selectivity for D-fructose because this carbohydrate forms the most stable boronate ester complex. The carbohydrate sensor is able to detect glucose in aqueous solution with a detection limit of about  $1\ \mu\text{M}$ .

A general approach to sensing enzyme activity is to utilize a covalently linked quencher–substrate complex (Q–S) that undergoes enzyme-catalyzed hydrolysis to release the quencher moiety, which has a strong effect on the CPE fluorescence. Using this approach, we have realized both fluorescence turn-off and turn-on systems to detect protease activity in aqueous solution; in the present review we only describe the turn-on assay (for further details, see reference [45]). Specifically, in the turn-on assay, the Q–S complex consists of a cationic peptide (the enzyme substrate) labeled with  $p$ -nitroanilide ( $p\text{-NA}$ , the quencher). The  $p\text{-NA}$  moiety is a strong fluorescence quencher for the anionic CPE  $\text{PPE-SO}_3$ , and the positive charge anchors the peptide to the polymer by electrostatic interactions. Because of this interaction, the  $p$ -

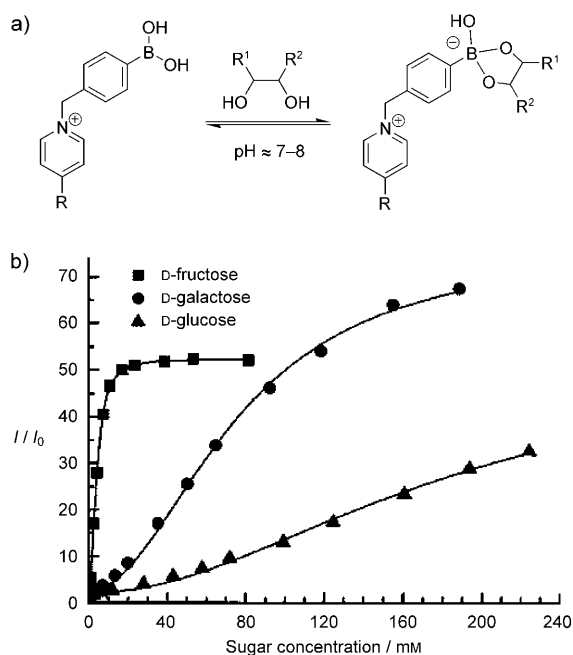


**Figure 10.** a) Interaction between boronic acid and sugar at almost neutral pH. b) Titration curves against sugar for the PPE-SO<sub>3</sub>/p-BV<sup>2+</sup> system. (Picture (b) from Ref. [80].)

NA-peptide conjugate quenches the fluorescence from PPE-SO<sub>3</sub> efficiently ( $K_{SV} \approx 10^6$ – $10^7$  M<sup>-1</sup>). In the presence of a proteolytic enzyme, such as peptidase, the *p*-NA-peptide is hydrolyzed and the *p*-NA unit is released. As this moiety is no longer charged, its ability to quench the polymer fluorescence is decreased substantially, resulting in an increase in fluorescence from PPE-SO<sub>3</sub> concomitant with peptide hydrolysis (Figure 11).

The last sensor that we describe involves coupling an enzyme-catalyzed hydrolysis reaction with a phospholipid substrate that strongly interacts with the CPE, modifying its physical state (aggregation and conformation) and fluorescence efficiency. Based on this principle, a fluorescence turn-off assay for the enzyme phospholipase C (PLC) was developed (Figure 12a).<sup>[44]</sup> In aqueous solution, negatively charged BpPPESO<sub>3</sub> (Figure 12b) exists predominantly in an aggregated state, showing weak, Stokes-shifted fluorescence. In the presence of a cationic phospholipid (10CPC), the BpPPESO<sub>3</sub> fluorescence intensity increases substantially owing to the formation of a CPE-phospholipid complex (on-state). The polymer fluorescence is enhanced because the phospholipid effectively disrupts aggregation of the CPE chains, eliminating the interchain interactions that induce fluorescence quenching. PLC catalyzes the hydrolysis of 10CPC (Figure 12b), leading to the formation of products that bind to BpPPESO<sub>3</sub> much less strongly. Thus, introduction of PLC into a solution containing CPE and 10CPC effectively disrupts the preformed CPE-phospholipid complex, causing the fluorescence intensity to decrease (off-state, Figure 12c). This sensitive PLC assay has an analytical detection limit for the enzyme of < 1 nM, and detailed kinetic studies show it to be a convenient, rapid, and real-time sensor for PLC activity.

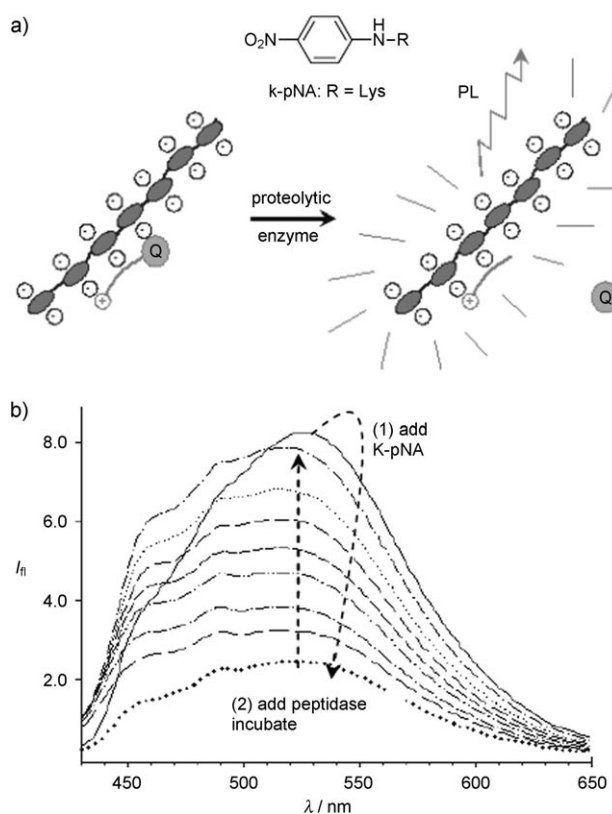


**Figure 11.** a) Structure of K-pNA and mechanism of turn-on assay for protease activity. b) Fluorescence changes during the assay: (—) initial fluorescence, (.....) after addition of K-pNA and with increasing incubation time after addition of peptidase.

## 6. Applications of Conjugated Polyelectrolytes in Optoelectronic Devices

One motivation for the molecular engineering of CPEs using various synthetic strategies revolves around their potential use in developing new generation optoelectronic devices. In contrast to conventional non-ionic conjugated polymers, CPEs can be dissolved in environmentally friendly solvents, such as water or alcohol, which has fuelled interest in their use in both devices and in biological applications. For devices, nanostructure control is of utmost importance; therefore, using CPEs in layer by layer (LbL) fashion allows the thickness to be precisely determined and thin films to be fabricated with optimized surface morphologies.

### 6.1. CPEs in Polymer Light-Emitting Diodes (PLEDs)

In 1996, Rubner and co-workers fabricated polymer light-emitting diodes (PLEDs) using LbL deposition of a cationic poly(phenylene-vinylene) (PPV) precursor-based active layer with that of oppositely charged nonconjugated polyelectrolytes (specifically poly(methacrylic acid) (PMA) or poly(styrenesulfonic acid) (PSS)), demonstrating molecular-level control over electrode interfaces and multilayer architecture.<sup>[82]</sup> In the LbL self-assembly, the polycationic sulfonium precursor of PPV was first manipulated into multilayers along with



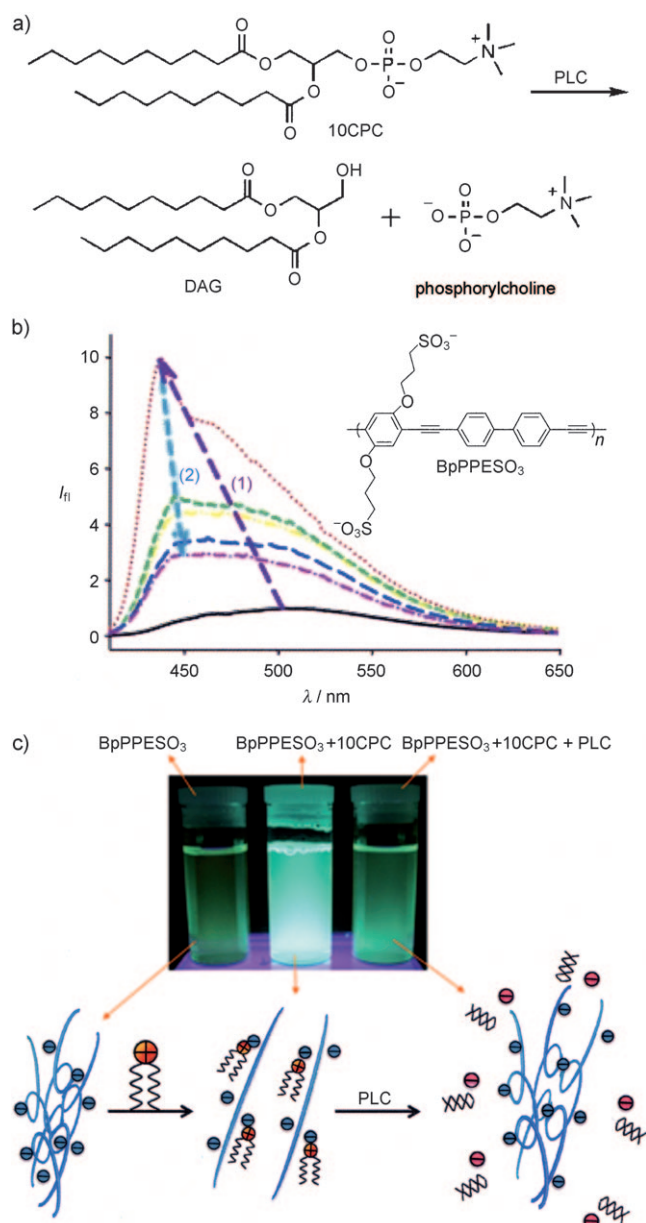


**Figure 12.** a) Hydrolysis of 10CPC by PLC. b) Fluorescence changes in the PLC turn-off assay: (—) initial fluorescence of BpPPESO<sub>3</sub>; (.....) after addition of 10CPC (step 1), and with increasing incubation time after addition of PLC (step 2). c) Mechanism of the PLC turn-off assay. (From Ref. [44].)

PMA or PSS. Subsequently, the sulfonium precursor form was thermally converted into the PPV, a light-emitting conjugated polymer, at 210°C. In particular, it was found that the acid strength of the anionic group plays an important role in determining the transport behavior of the PPV/polyanion bilayers. The light-voltage ( $L$ - $V$ ) and current-voltage ( $I$ - $V$ ) curves obtained from 20 bilayers of either the PMA/PPV or PPS/PPV system shows that the PMA/PPV devices delivered much higher luminescence levels than the PSS/PPV devices. The PMA/PPV device was found to typically operate at 10–50  $\text{cd m}^{-2}$ , whereas the PSS/PPV devices produced only about 1  $\text{cd m}^{-2}$ .

Shortly thereafter, we reported that combined anionic and cationic water-soluble (+/–) PPP polyelectrolytes having identical conjugated backbone structures (Figure 13a) could

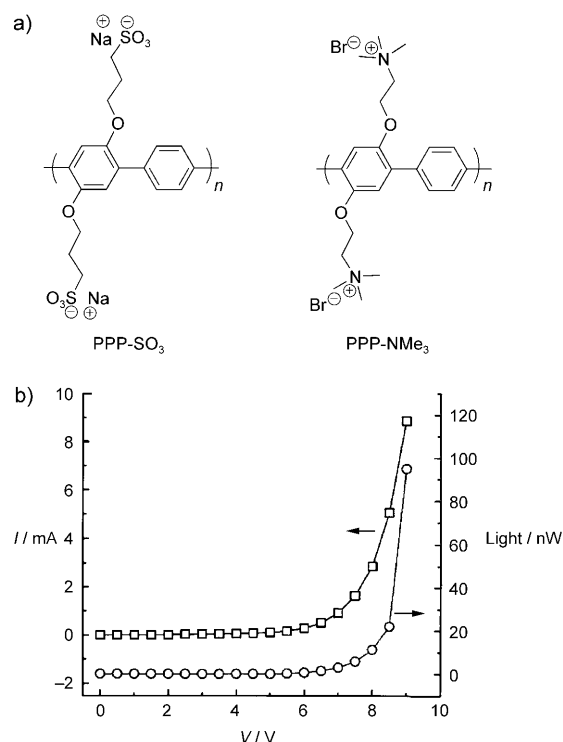


**Figure 13.** a) Structures of PPP-based CPEs used as alternating layers in PLED studies. b) Device current and light output as a function of applied voltage for a 35-bilayer, 21 nm thick (+/–) PPP film. (From Ref. [83].)

be readily processed into multilayer thin-film light-emitting devices using the LbL sequential adsorption technique.<sup>[83]</sup> Using one type of alternating conjugated backbone showed a relatively low turn-on voltage (7 V) and improved external quantum efficiencies ( $2 \times 10^{-3}\%$ ; Figure 13b) compared to devices where the active layer was alternated with ionic nonconjugated polyelectrolytes.

Although this early study demonstrated the use of a consistent conjugated backbone, the ability to use heterostructured systems with different molecular compositions could expand the possibilities of property control. In a demonstration of such a possibility, in 2005, Bazan, Heeger and co-workers fabricated a multilayer heterostructure using a fluorene-based copolymer, PFO-PBD-NMe<sub>3</sub><sup>+</sup>, as an electron transport layer along with PEDOT:PSS as a hole transport layer within the PLED.<sup>[84]</sup> The emissive layer (PFO or MEH-PPV) was spin-coated from an organic solvent followed by PFO-PBD-NMe<sub>3</sub><sup>+</sup> spin-coated from methanol, preventing the disruption of the underlying emissive layer that is insoluble in alcohols. The PLED device with a configuration of ITO/PEDOT:PSS/emissive layer/PFO-PBD-NMe<sub>3</sub><sup>+</sup>/Ba/Al was constructed. The device operated at a very low turn-on voltage (ca. 3 V) owing to utilization of the electron transport layer. At 6 V, the emissive layer/electron transport layer (PFO-PBD-NMe<sub>3</sub><sup>+</sup>) configuration displayed a

brightness of  $3450 \text{ cd m}^{-2}$  compared to  $30 \text{ cd m}^{-2}$  for the device without the electron transport layer. Despite this successful application of CPEs as electron transport layers, the exact mechanism by which electron injection occurs remains unclear. Some progress towards understanding the effect was made recently by Bazan and co-workers in a study that suggests that ion motion in the CPE layer affects the overall device performance.<sup>[85,86]</sup> In that study, the nature of the charge-compensating ion significantly influences the turn-on voltage and efficiency of the device.

## 6.2. CPEs in Photovoltaic Devices

Polymer-based photovoltaic (PV) cells are of significant interest as they offer the possibility of lightweight, shape-variable, and potentially cost-effective solutions to solar energy conversion.<sup>[87]</sup> There has been considerable interest in the construction of photovoltaic cells in which the active matrix consists of a semiconducting conjugated polymer based on donor–acceptor bulk heterojunctions that are designed for efficient current collection.<sup>[87–89]</sup> The synthesis of the active polymer matrix is carefully engineered to accommodate various factors, such as exciton diffusion, charge-carrier generation and transport, and open-circuit voltage, which directly affect the photovoltaic efficiency. The key requirement is to maintain control of the nanostructure through the choice of repeat unit and macromolecular structure of the components. Several groups have thus used CPEs to either apply LbL or hybrid approaches to constructing photovoltaic cells.

The use of CPEs in solar cells was fueled by a report from Baur et al. in which a photovoltaic device was constructed by the LbL method.<sup>[90]</sup> The cationic PPV precursor as a light acceptor and electron donor was alternated with an anionic  $\text{C}_{60}$  derivative, which acts as an acceptor. Despite the novelty of this work, the overall power conversion efficiency was low. For five PPV/ $\text{C}_{60}$  bilayers, the short-circuit current ( $I_{\text{sc}}$ ) and open-circuit voltage ( $V_{\text{oc}}$ ) were 150 nA and 0.4 V, respectively, and was attributed to several factors, including a low optical cross-section in the visible region combined with poor carrier mobilities within the LbL film.<sup>[90]</sup>

In 2005, we used LbL fabrication of multilayer films to construct photovoltaic cells using PPE-based anionic conjugated polyelectrolytes as electron donors and a water-soluble cationic fullerene  $\text{C}_{60}$  derivative as the acceptor (Figure 14).<sup>[91]</sup> The efficiency of the film was linearly related to the number of bilayers, as indicated by UV/Vis spectroscopy. The maximum incident monochromatic photon-to-current conversion efficiency (IPCE) of the photovoltaic cells was 5.5 %.

These cells have open-circuit voltages of 200–250 mV, with the highest measured short-circuit currents of up to  $0.5 \text{ mA cm}^{-2}$  and fill factors of around 30 %. The power conversion efficiencies measured at AM1.5 simulated solar conditions ( $100 \text{ mW cm}^{-2}$ ) varied between 0.01 and 0.04 %, and, as with the IPCE results, the efficiency is a function of the thickness of the PV active layer.<sup>[91]</sup> Although the overall power conversion efficiency of the cells under simulated solar light was relatively low, this result is the best conversion

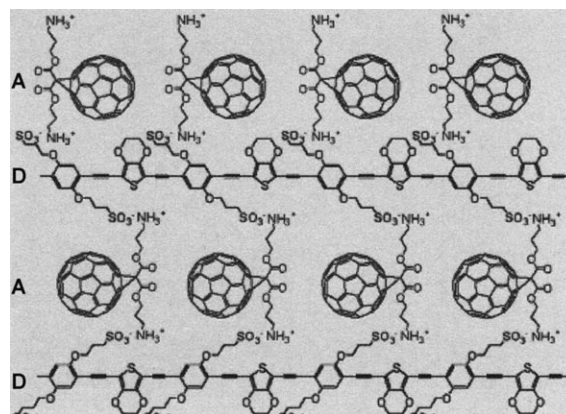


**Figure 14.** The alternating donor (PPE-EDOT- $\text{SO}_3^-$ ) and acceptor ( $\text{C}_{60}\text{-NH}_3^+$ ) layers forming the active material of a photovoltaic device. (From Ref. [91].)

efficiency for photovoltaic cells constructed using the LbL approach.

Shortly afterwards, we demonstrated the concept of spectral broadening by using a dual-polymer system in a polymer-sensitized  $\text{TiO}_2$  solar cell.<sup>[42]</sup> The photocurrent was generated by photoinduced electron transfer at the interface between the sensitizer polymers (PPE- $\text{CO}_2$ , **12** in Scheme 4, and PT- $\text{CO}_2$ ) and the acceptor,  $\text{TiO}_2$ , within the hybrid cells. For both polymers, the LUMO levels are energetically higher than the conduction band of  $\text{TiO}_2$ , and therefore charge injection into  $\text{TiO}_2$  by the singlet excited state of the polymers is energetically favorable, which is supported by transient absorption studies. As a result, the photocurrent ( $2.7 \text{ mA cm}^{-2}$ ) and  $\eta$  (ca. 0.9 %) obtained for the dual-polymer solar cell was essentially the sum of the response from each individual polymer (Figure 15).

Although the cells reported herein were not optimized with respect to factors such as concentration of the polymer solution and film thickness, these results demonstrated the potential for using CPEs as sensitizers in nanocrystalline  $\text{TiO}_2$  hybrid solar cells. By synthesizing CPEs with absorption further into the long-wavelength (red and NIR) region, the spectral broadening could be expanded, leading to a close matching of the full solar spectrum.

Recently we have worked towards this objective using a series of poly(arylene-ethynylene) conjugated polyelectrolytes substituted with carboxylic acid side groups (Figure 16a).<sup>[92]</sup> The PPE-based CPEs contain a second arylene-ethynylene moiety of variable electron demand, yielding a HOMO–LUMO gap that varies, leading to absorption maxima ranging from 404 to 495 nm. Exposure of  $\text{TiO}_2$  films to solutions of the CPEs leads to adsorption of the polymers onto the semiconductor surface, with coverage sufficient to give rise to more than 90 % light absorption at wavelengths corresponding to the band maximum of the polymers. The  $\text{TiO}_2$ /CPE films were evaluated in a dye-sensitized solar cell (DSSC) configuration using an  $\text{I}_3^-/\text{I}^-$  propylene carbonate electrolyte and Pt/FTO counter electrode. For each CPE, the photocurrent action spectra match the absorption spectra well, with IPCE approaching 50 % at

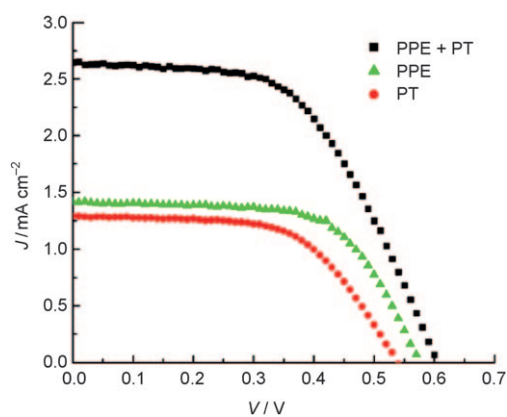


**Figure 15.** *J*–*V* characteristics under AM1.5 conditions for solar cells sensitized with PPE-CO<sub>2</sub>, PT-CO<sub>2</sub>, and PPE-CO<sub>2</sub>/PT-CO<sub>2</sub>. (From Ref. [42].)

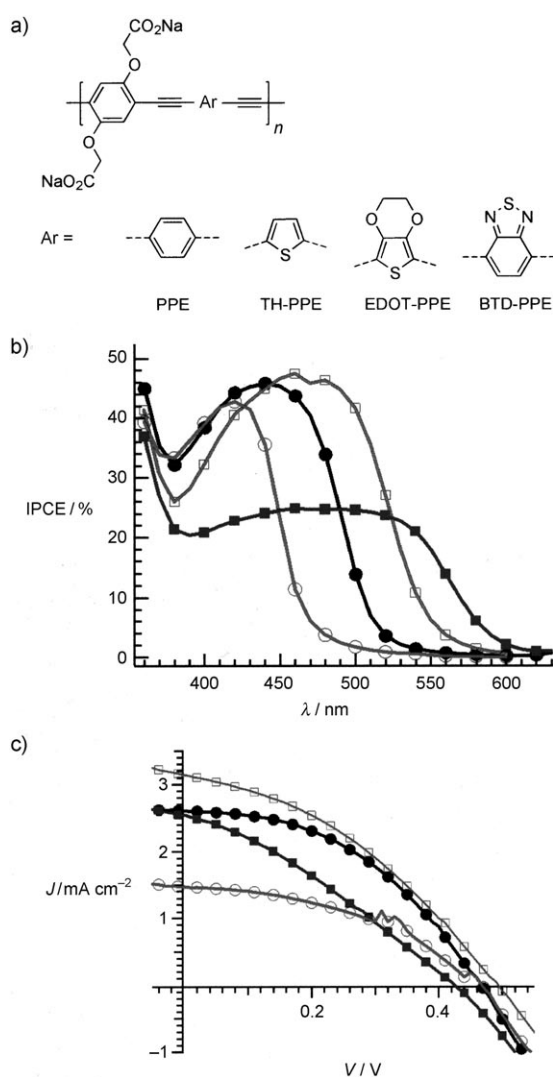


**Figure 16.** a) Structures of the repeat units for variable-gap PPE-based CPEs used in TiO<sub>2</sub>-sensitized photovoltaic devices. b) Photocurrent action spectra of CPE-sensitized solar cells. c) *J*–*V* characteristics of CPE-sensitized solar cells under AM1.5 conditions. (○) PPE, (●) TH-PPE, (□) EDOT-PPE, (■) BTDP-PPE. (From Ref. [92].)

the absorption maxima for the CPEs (Figure 16b). The photocurrent and power conversion efficiency (Figure 16c) under AM1.5 illumination increases in the order PPE < TH-PPE < EDOT-PPE, which is consistent with the red-shift in the polymer absorption. A curious feature is the fact that the IPCE and power conversion efficiency for the TiO<sub>2</sub>/BTDP-PPE system is substantially less than those for the other CPEs, and the decreased efficiency is attributed to exciton trapping in polymer aggregates; the excitons are present in the film, but separated from the TiO<sub>2</sub> interface.

In general, the linear CPEs rely on pendant-group steric interactions and conjugation breaks to disrupt the structures and to prevent aggregation. Such a disrupted state can also be created by incorporating three-dimensional structures, such as dendrimers or hyperbranched polymers (HBPs). HBPs offer an advantage over dendrimers because of their ease of synthesis in a single reaction. In 2007, we reported an investigation involving the use of ionic conjugated hyperbranched polymer materials (HBP-CPEs) as sensitizers for TiO<sub>2</sub>-based photovoltaic cells.<sup>[59]</sup> Both anionic (**22a**) and cationic (**22b**) HBP-CPEs (Scheme 8) were adsorbed onto porous TiO<sub>2</sub> to produce monolayer and bilayer self-assembled films (red and yellow dots in Figure 17a). The self-assembly, driven by ionic interactions of oppositely charged HBP-CPEs, results in an increased chromophore concentration.

As shown by the IPCE and power conversion results, bilayer formation led to enhanced optical density and more efficient light harvesting in the hybrid cells. Studies were carried out to explore the effects of deposition sequence (cationic CPE followed by anionic CPE, or vice versa) on the film properties and photoelectrochemical cell efficiencies. The results show that both IPCE and overall cell performance are higher for a bilayer configuration compared to monolayer films (Figure 17b) and that although initial deposition of the

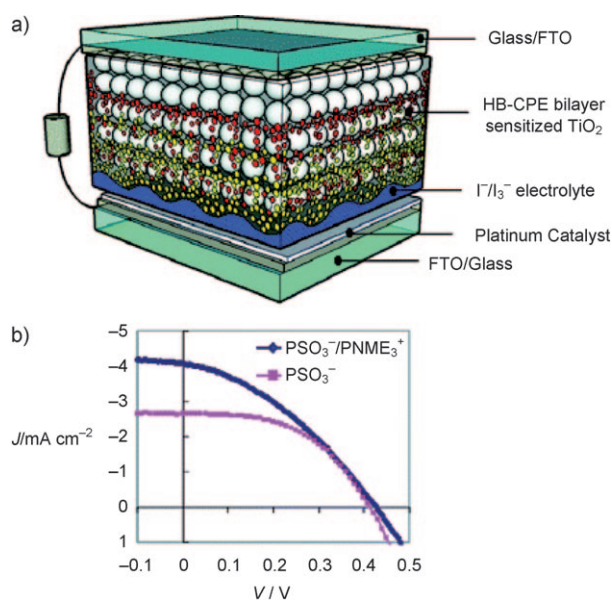


**Figure 17.** a) A bilayer solar cell sensitized with HB-CPE. b) *J*–*V* curves for a monolayer and self-assembled bilayer (with PSO<sub>3</sub><sup>−</sup> as the first layer) under AM1.5 conditions. (From Ref. [59].)



anionic polymer led to enhanced cell characteristics, the overall improvement was minimal.

## 7. Summary and Outlook

This review provides an overview of the synthesis, properties, and applications of organic conjugated polyelectrolytes. In the relatively short period since these materials were first developed, a large number of systems have been synthesized and their properties characterized, and applications have been explored that range from biosensors to optoelectronic devices. The unique nature of CPEs (such as strong and tunable absorption and photoluminescence, semiconductor properties) stems from the functionality of the  $\pi$ -conjugated backbone combined with the ionic side groups that impart the materials with solubility in and the ability to process from aqueous solutions.

Conjugated polyelectrolytes clearly show strong promise for use in a number of commercially viable applications. Application development is facilitated by availability of materials, and as shown in the first sections of the review, there are a number of CPEs that are available by relatively efficient and straightforward synthetic paths. This fact suggests that in the near future, specific CPEs will be available from commercial sources. This will undoubtedly drive further innovation in the field, as scientists who are unable to carry out synthetic chemistry will have access to CPEs for research and development work.

In our view, one of the most promising applications for CPEs is as biosensors for nucleic acids or for enzyme activity assays. The work done to date in this area has focused mainly on demonstrating the feasibility of carrying out these assays. Further work in this area will need to focus on integrating the sensor systems into high throughput screening formats that are typically used by the biotechnology industry in drug development.

We believe strongly that CPEs represent one of the most interesting and useful classes of conjugated polymers. Although the area has seen significant development already, there are a number of promising areas that are ripe for further development and use in specific applications. This review highlights some of these areas, and points the way to future developments in the field.

*We acknowledge the United States Department of Energy, Office of Basic Energy Sciences (DE-FG-02-96ER14617) for support of this work. K.S.S. and J.R.R. gratefully acknowledge the contributions that our many students, postdoctoral fellows, and collaborators have made to our CPE-related research projects over the years.*

Received: November 7, 2008  
Published online: May 14, 2009

- [1] *Handbook of Conducting Polymers*, Vol. 1, 3rd ed. (Eds.: T. A. Skotheim, J. R. Reynolds), CRC, Boca Raton, FL, **2007**.

- [2] *Handbook of Conducting Polymers*, Vol. 2, 3rd ed. (Eds.: T. A. Skotheim, J. R. Reynolds), CRC, Boca Raton, FL, **2007**.  
[3] M. R. Pinto, K. S. Schanze, *Synthesis* **2002**, 1293–1309.  
[4] H. A. Ho, A. Najari, M. Leclerc, *Acc. Chem. Res.* **2008**, *41*, 168–178.  
[5] S. J. Dwight, B. S. Gaylord, J. W. Hong, G. C. Bazan, *J. Am. Chem. Soc.* **2004**, *126*, 16850–16859.  
[6] K. S. Schanze, X. Zhao in *Handbook of Conducting Polymers*, Vol. 1, 3rd ed. (Eds.: T. A. Skotheim, J. R. Reynolds), CRC, Boca Raton, FL, **2007**, pp. 14.01–14.29.  
[7] P. Nilsson, O. Inganäs in *Handbook of Conducting Polymers*, Vol. 2, 3rd ed. (Eds.: T. A. Skotheim, J. R. Reynolds), CRC, Boca Raton, FL, **2007**, pp. 13.01–13.24.  
[8] S. W. Thomas III, G. D. Joly, T. M. Swager, *Chem. Rev.* **2007**, *107*, 1339–1386.  
[9] B. Liu, G. C. Bazan, *Chem. Mater.* **2004**, *16*, 4467–4476.  
[10] K. E. Achyuthan, T. S. Bergstedt, L. Chen, R. M. Jones, S. Kumaraswamy, S. A. Kushon, K. D. Ley, L. Lu, D. McBranch, H. Mukundan, F. Rininsland, X. Shi, W. Xia, D. G. Whitten, *J. Mater. Chem.* **2005**, *15*, 2648–2656.  
[11] C. V. Hoven, A. Garcia, G. C. Bazan, T.-Q. Nguyen, *Adv. Mater.* **2008**, *20*, 3793–3810.  
[12] A. O. Patil, Y. Ikenoue, F. Wudl, A. J. Heeger, *J. Am. Chem. Soc.* **1987**, *109*, 1858–1859.  
[13] N. S. Sundaresan, S. Basak, M. Pomerantz, J. R. Reynolds, *J. Chem. Soc. Chem. Commun.* **1987**, 621–622.  
[14] J. R. Reynolds, N. S. Sundaresan, M. Pomerantz, S. Basak, C. K. Baker, *J. Electroanal. Chem. Interfacial Electrochem.* **1988**, *250*, 355–371.  
[15] P. Schottland, O. Fichet, D. Teyssie, C. Chevrot, *Synth. Met.* **1999**, *101*, 7–8.  
[16] C. A. Cutler, M. Bouguettaya, T.-S. Kang, J. R. Reynolds, *Macromolecules* **2005**, *38*, 3068–3074.  
[17] T. I. Wallow, B. M. Novak, *J. Am. Chem. Soc.* **1991**, *113*, 7411–7412.  
[18] P. Kovacic, M. B. Jones, *Chem. Rev.* **1987**, *87*, 357–379.  
[19] I. U. Rau, M. Rehahn, *Polymer* **1993**, *34*, 2889–2893.  
[20] V. Chaturvedi, S. Tanaka, K. Kaeriyama, *Macromolecules* **1993**, *26*, 2607–2611.  
[21] M. Ueda, M. Yoneda, *Macromol. Rapid Commun.* **1995**, *16*, 469–475.  
[22] R. Rulkens, M. Schulze, G. Wegner, *Macromol. Rapid Commun.* **1994**, *15*, 669–676.  
[23] A. D. Child, J. R. Reynolds, *Macromolecules* **1994**, *27*, 1975–1977.  
[24] S. Kim, J. Jackiw, E. Robinson, K. S. Schanze, J. R. Reynolds, J. Baur, M. F. Rubner, D. Boils, *Macromolecules* **1998**, *31*, 964–974.  
[25] G. Brodowski, A. Horvath, M. Ballauff, M. Rehahn, *Macromolecules* **1996**, *29*, 6962–6965.  
[26] M. Wittemann, M. Rehahn, *Chem. Commun.* **1998**, 623–624.  
[27] B. S. Harrison, M. B. Ramey, J. R. Reynolds, K. S. Schanze, *J. Am. Chem. Soc.* **2000**, *122*, 8561–8562.  
[28] Q. Zhou, T. M. Swager, *J. Am. Chem. Soc.* **1995**, *117*, 7017–7018.  
[29] M. B. Ramey, J.-A. Hiller, M. F. Rubner, C. Tan, K. S. Schanze, J. R. Reynolds, *Macromolecules* **2005**, *38*, 234–243.  
[30] S. Shi, F. Wudl, *Macromolecules* **1990**, *23*, 2119–2124.  
[31] L. Chen, D. W. McBranch, H.-L. Wang, R. Helgeson, F. Wudl, D. G. Whitten, *Proc. Natl. Acad. Sci. USA* **1999**, *96*, 12287–12292.  
[32] Z. Gu, Y. Bao, Y. Zhang, M. Wang, Q. Shen, *Macromolecules* **2006**, *39*, 3125–3131.  
[33] Z. Peng, B. Xu, J. Zhang, Y. Pan, *Chem. Commun.* **1999**, 1855–1856.  
[34] U. H. F. Bunz, *Acc. Chem. Res.* **2001**, *34*, 998–1010.  
[35] T. M. Swager, C. J. Gil, M. S. Wrighton, *J. Phys. Chem.* **1995**, *99*, 4886–4893.



- [36] C. Li, W. T. Slaven IV, V. T. John, S. Banerjee, *Chem. Commun.* **1997**, 1569–1570.
- [37] W. T. Slaven IV, C. Li, Y. Chen, V. T. John, S. H. Rachakonda, *J. Mater. Sci. Pure Appl. Chem.* **1999**, A36, 971–980.
- [38] T. M. Swager, *Acc. Chem. Res.* **1998**, 31, 201–207.
- [39] C. Tan, M. R. Pinto, K. S. Schanze, *Chem. Commun.* **2002**, 446–447.
- [40] C. Tan, E. Atas, J. G. Muller, M. R. Pinto, V. D. Kleiman, K. S. Schanze, *J. Am. Chem. Soc.* **2004**, 126, 13685–13694.
- [41] M. R. Pinto, B. M. Kristal, K. S. Schanze, *Langmuir* **2003**, 19, 6523–6533.
- [42] J. K. Mwaura, X. Zhao, H. Jiang, K. S. Schanze, J. R. Reynolds, *Chem. Mater.* **2006**, 18, 6109–6111.
- [43] X. Zhao, K. S. Schanze, *Langmuir* **2006**, 22, 4856–4862.
- [44] Y. Liu, K. Ogawa, K. S. Schanze, *Anal. Chem.* **2008**, 80, 150–158.
- [45] M. R. Pinto, K. S. Schanze, *Proc. Natl. Acad. Sci. USA* **2004**, 101, 7505–7510.
- [46] Y. Liu, K. S. Schanze, *Anal. Chem.* **2008**, 80, 8605–8612.
- [47] Y. Liu, K. S. Schanze, *Anal. Chem.* **2009**, 81, 231–239.
- [48] X. Zhao, M. R. Pinto, L. M. Hardison, J. Mwaura, J. Muller, H. Jiang, D. Witker, V. D. Kleiman, J. R. Reynolds, K. S. Schanze, *Macromolecules* **2006**, 39, 6355–6366.
- [49] K. Haskins-Glusac, M. R. Pinto, C. Tan, K. S. Schanze, *J. Am. Chem. Soc.* **2004**, 126, 14964–14971.
- [50] B. Liu, W. Yu, Y. Lai, W. Huang, *Macromolecules* **2002**, 35, 4975–4982.
- [51] B. S. Gaylord, A. J. Heeger, G. C. Bazan, *J. Am. Chem. Soc.* **2003**, 125, 896–900.
- [52] F. Huang, L. Hou, H. Wu, X. Wang, H. Shen, W. Cao, W. Yang, Y. Cao, *J. Am. Chem. Soc.* **2004**, 126, 9845–9853.
- [53] H. D. Burrows, V. M. M. Lobo, J. Pina, M. L. Ramos, J. Seixas de Melo, A. J. M. Valente, M. J. Tapia, S. Pradhan, U. Scherf, *Macromolecules* **2004**, 37, 7425–7427.
- [54] M. Knaapila, L. Almasy, V. M. Garamus, C. Pearson, S. Pradhan, M. C. Petty, U. Scherf, H. D. Burrows, A. P. Monkman, *J. Phys. Chem. B* **2006**, 110, 10248–10257.
- [55] R. N. Brookins, K. S. Schanze, J. R. Reynolds, *Macromolecules* **2007**, 40, 3524–3526.
- [56] S. W. Wright, D. L. Hageman, L. D. McClure, *J. Org. Chem.* **1994**, 59, 6095–6097.
- [57] S. Wang, J. W. Hong, G. C. Bazan, *Org. Lett.* **2005**, 7, 1907–1910.
- [58] B. Zhu, Y. Han, M. Sun, Z. Bo, *Macromolecules* **2007**, 40, 4494–4500.
- [59] P. Taranekar, Q. Qiao, H. Jiang, I. Ghiviriga, K. S. Schanze, J. R. Reynolds, *J. Am. Chem. Soc.* **2007**, 129, 8958–8959.
- [60] H. Jiang, X. Zhao, K. S. Schanze, *Langmuir* **2006**, 22, 5541–5543.
- [61] P. Kaur, H. Yue, M. Wu, M. Liu, J. Treece, D. H. Waldeck, C. Xue, H. Liu, *J. Phys. Chem. B* **2007**, 111, 8589–8596.
- [62] H. Jiang, X. Zhao, K. S. Schanze, *Langmuir* **2007**, 23, 9481–9486.
- [63] C. Tan, M. R. Pinto, M. E. Kose, I. Ghiviriga, K. S. Schanze, *Adv. Mater.* **2004**, 16, 1208–1212.
- [64] J. C. Nelson, J. G. Saven, J. S. Moore, P. G. Wolynes, *Science* **1997**, 277, 1793–1796.
- [65] R. B. Prince, J. G. Saven, P. G. Wolynes, J. S. Moore, *J. Am. Chem. Soc.* **1999**, 121, 3114–3121.
- [66] S. Lahiri, J. L. Thompson, J. S. Moore, *J. Am. Chem. Soc.* **2000**, 122, 11315–11319.
- [67] Q. Zhou, T. M. Swager, *J. Am. Chem. Soc.* **1995**, 117, 12593–12602.
- [68] J. R. Lakowicz, *Principles of Fluorescence Spectroscopy*, 2nd ed., Kluwer Academic/Plenum Publishers, New York, **1999**.
- [69] J. G. Muller, E. Atas, C. Tan, K. S. Schanze, V. D. Kleiman, *J. Am. Chem. Soc.* **2006**, 128, 4007–4016.
- [70] D. L. Wang, X. Gong, P. S. Heeger, F. Rininsland, G. C. Bazan, A. J. Heeger, *Proc. Natl. Acad. Sci. USA* **2002**, 99, 49–53.
- [71] B. S. Gaylord, A. J. Heeger, G. C. Bazan, *Proc. Natl. Acad. Sci. USA* **2002**, 99, 10954–10957.
- [72] O. R. Miranda, C. C. You, R. Phillips, I. B. Kim, P. S. Ghosh, U. H. F. Bunz, V. M. Rotello, *J. Am. Chem. Soc.* **2007**, 129, 9856–9857.
- [73] L. L. An, S. Wang, D. B. Zhu, *Chem. Asian J.* **2008**, 3, 1601–1606.
- [74] F. D. Feng, Y. L. Tang, F. He, M. H. Yu, X. R. Duan, S. Wang, Y. H. Li, D. B. Zhu, *Adv. Mater.* **2007**, 19, 3490–3495.
- [75] F. D. Feng, Y. L. Tang, S. Wang, Y. L. Li, D. B. Zhu, *Angew. Chem.* **2007**, 119, 8028–8032; *Angew. Chem. Int. Ed.* **2007**, 46, 7882–7886.
- [76] F. He, Y. L. Tang, M. H. Yu, S. Wang, Y. L. Li, D. B. Zhu, *Adv. Funct. Mater.* **2006**, 16, 91–94.
- [77] Y. L. Tang, F. Teng, M. H. Yu, L. L. An, F. He, S. Wang, Y. L. Li, D. B. Zhu, G. C. Bazan, *Adv. Mater.* **2008**, 20, 703–705.
- [78] F. He, F. Feng, S. Wang, Y. L. Li, D. B. Zhu, *J. Mater. Chem.* **2007**, 17, 3702–3707.
- [79] X. Zhao, Y. Liu, K. S. Schanze, *Chem. Commun.* **2007**, 2914–2916.
- [80] N. DiCesare, M. R. Pinto, K. S. Schanze, J. R. Lakowicz, *Langmuir* **2002**, 18, 7785–7787.
- [81] C. J. Yang, M. Pinto, K. Schanze, W. Tan, *Angew. Chem.* **2005**, 117, 2628; *Angew. Chem. Int. Ed.* **2005**, 44, 2572–2576.
- [82] O. Onitsuka, A. C. Fou, M. Ferreira, B. R. Hsieh, M. F. Rubner, *J. Appl. Phys.* **1996**, 80, 4067–4071.
- [83] J. W. Baur, S. Kim, P. B. Balanda, J. R. Reynolds, M. F. Rubner, *Adv. Mater.* **1998**, 10, 1452–1455.
- [84] W. Ma, P. K. Iyer, X. Gong, B. Liu, D. Moses, G. C. Bazan, A. J. Heeger, *Adv. Mater.* **2005**, 17, 274–277.
- [85] C. Hoven, R. Yang, A. Garcia, A. J. Heeger, T.-Q. Nguyen, G. C. Bazan, *J. Am. Chem. Soc.* **2007**, 129, 10976–10977.
- [86] R. Yang, Y. Xu, X.-D. Dang, T.-Q. Nguyen, Y. Cao, G. C. Bazan, *J. Am. Chem. Soc.* **2008**, 130, 3282–3283.
- [87] J. C. Brabec, *Sol. Energy Mater. Sol. Cells* **2004**, 83, 273–292.
- [88] N. S. Sariciftci, L. Smilowitz, A. J. Heeger, F. Wudl, *Science* **1992**, 258, 1474–1476.
- [89] *Organic Photovoltaics: Concepts and Realization* (Eds.: J. C. Brabec, V. Dyakonov, J. Parisi, N. S. Sariciftci), Springer, Berlin, **2003**.
- [90] J. W. Baur, M. F. Durstock, B. E. Taylor, R. J. Spry, S. Reulbach, L. Y. Chiang, *Synth. Met.* **2001**, 121, 1547–1548.
- [91] J. K. Mwaura, M. R. Pinto, D. Witker, N. Ananthakrishnan, K. S. Schanze, J. R. Reynolds, *Langmuir* **2005**, 21, 10119–10126.
- [92] H. Jiang, X. Zhao, A. H. Shelton, S. H. Lee, J. R. Reynolds, K. S. Schanze, *ACS Appl. Mater. Interfaces* **2009**, 1, 381–387.